Tibio-femoral joint contact mechanics: An in-vitro simulation with a 6 DOF static knee simulator

Paul Gauthier, BSc PT

Committee Members: Mario Lamontagne, Ph.D.
Geoffrey Dervin, MD

Supervisor: Daniel Benoit (PhD)

Thesis

A Thesis Submitted in Partial Fulfillment of the Requirements for the Degree of Master of Science in Human Kinetics

School of Human Kinetics
Faculty of Health Sciences
University of Ottawa

December 2016

Abstract

Introduction: Understanding the relationship between muscle loads crossing the knee joint and knee joint mechanics is critical for understanding knee stability and the effects of altered muscle forces on healthy and ACL injured knees. In vitro measurement can be used to elucidate this if the simulation is biofidelic, allowing the physiological levels of applied loads to dictate the tibiofemoral kinematics in all degrees of freedom (DoF). The objectives of this study were to describe and apply the University of Ottawa knee simulator as well as measure the reliability of the device. In addition, this device was used to quantify the effect of muscle loads and anterior cruciate ligament (ACL) resection on contact mechanics and kinematics of the tibiofemoral joint. Methods: Muscle forces were determined from an electromyography-driven musculoskeletal model of a healthy male during gait. Six knee specimens were loaded into the simulator and subjected to 100%, 75% and 50% in vivo muscle forces applied through the 6 simulated muscles, in addition to a quadriceps weakness and a hamstring weakness condition. Tibiofemoral mechanics were measured with all 5 loading conditions before and after ACL transection. Results: With the ACL intact, very high reliability in contact area and pressures among loading conditions were observed as the intra-class correlation coefficients (ICC) ranged from 0.932 to 0.99. After ACL transection, reliability remained very high as ICCs ranged from 0.926 to 0.99. In all simulated conditions, muscle forces maintained the knee joint in a stable position resulting in minimal kinematic differences, but altered contact mechanics in both the ACL and non-ACL condition. Removal of the ACL significantly reduced both the medial and lateral contact areas in all loading conditions compared to the ACL intact condition. Conclusion: In summary, the UOKS has demonstrated high reliability within repeated measures. Additionally, small, normally undetectable alterations in joint kinematics resulted in significant alterations to contact mechanics, which can be linked to the degenerative process.

Table of Contents

Introduction

The economic burden of musculoskeletal conditions in Canada accounted for 10.3% of the total economic burden of all diseases but only 1.3% of health science research (The Arthritis Society). This disproportion may explain why there is limited information on the underlying causes of knee osteoarthritis (OA). OA is characterized by the degeneration of the articular surfaces, the formation of osteophytes and the reduction of joint space, further leading to pain, swelling, and limited range of motion (The Arthritis Society). The Arthritis Society states that many risk factors have been associated with the development of OA including: age, family history, excess weight, and previous injury. However, there is an emerging consensus that mechanical factors play a significant role in the alteration of joint integrity over time and this may play a part in the development of OA (Asano T, 2001).

Andriacchi and colleagues (2004) (Andriacchi et al., 2004) suggested that a shift in functional load bearing contact areas coupled with rotational misalignment leads to degradation of the cartilage (see Appendix 1). Also, joint degeneration has been related to load magnitudes as reported by Riegger-Krugh (1998) that correlated tibiofemoral joint degeneration with excessive joint contact pressures. Excessive joint loads can be produced by abnormally high loading during sports, high-rate loading, a forceful gait pattern, or misalignment of the knee (Radin, Yang, Riegger, Kish, & O'Connor, 1991; Riegger-Krugh et al., 1998). Thus, the incidence, magnitude and pathogenesis of knee OA depend on the individual's daily activities and the joint loading involved. Therefore, studying healthy knee joint mechanics as they relate to functional loading may provide valuable insight into the underlying mechanisms of OA development and progression.

For obvious ethical and logistical reasons, it is very difficult to study all aspects of the intra-articular mechanics of the knee. In-vivo studies are invasive and complex (D'Lima, Steklov, Fregly, Banks, & Colwell Jr., 2008; Glitsch & Baumann, 1997; Heinlein, Graichen, Bender, Rohlmann, & Bergmann, 2007; Mündermann, Dyrby, D'Lima, Colwell Jr., & Andriacchi, 2008; Taylor & Walker, 2001). For this reason, several investigations have used cadaver knee specimens and artificial knees with a variety of knee simulators to mimic in-vitro knee kinetics and kinematics, in order to further our understanding of knee contact mechanics (Kainz, Reng, Augat, & Wurm, 2011; Lee et al., 2006; Maletsky & Hillberry, 2005; Marzo & Gurske-DePerio, 2009; Riegger-Krugh et al., 1998; Werner, Ayers, Maletsky, & Rullkoetter, 2005; Wünschel, Leichtle, Obloh, Wülker, & Müller, 2011).

In recent literature, notable variables studied were: mean contact area, mean contact stress, peak contact stress, and joint contact pressures (Lee et al., 2006). Interestingly, excessive joint contact pressure is identified as a contributing factor in the pathogenesis of degenerative joint disease (Herzog & Longino, 2007; Riegger-Krugh et al., 1998)

Many studies have investigated the effects of meniscus and ligamentous derangements and repairs, knee arthroplasties (total and unilateral), and general surgical outcomes on joint pressures and overall joint mechanics (Briem, Ramsey, Newcomb, Rudolph, & Snyder-Mackler, 2007; Fukubayashi & Kurosawa, 1980; Ihn, Kim, & Park, 1993; Jeffcote, Nicholls, Schirm, & Kuster, 2007; Lee et al., 2006; Lewold, Robertsson, Knutson, & Lidgren, 1998; Li, Moses, Papannagari, Pathare, DeFrate, & Gill, 2006a; Li et al., 2007; Liau, Cheng, Huang, & Lo, 2002; Perillo-Marcone & Taylor, 2007; Poh et al., ; Ramsey, Snyder-Mackler, Lewek, Newcomb, & Rudolph, 2007; Seo et al., 2009; Van De Velde et al., 2009; Varadarajan, Moynihan, D'Lima, Colwell, & Li, 2008; Yoo et al., 2005) . However, the actual individual muscle contributions to joint loads were not included in these evaluations, thus, the effects of individual muscle force on

the tibiofemoral contact mechanics has not been measured. Knee contact mechanics are governed by three components: (1) articular geometry, which encompasses bony and cartilaginous structures; (2) passive constraints such as ligaments fascia and capsule; (3) and neuromuscular control of the loads applied to the knee through weight bearing and muscle tension (Williams et al., 2001; Williams, Chmielewski, Rudolph, Buchanan, & Snyder-Mackler, 2001). Now considering that muscles are the only dynamic actuators of knee joint loads and are suggested to be the most important contributor (Herzog & Longino, 2007), investigation of contact mechanics of the tibiofemoral joint with a simulation of physiologically representative muscle force is warranted. One objective of this study will be to determine the effects of different muscle force profiles on the tibiofemoral contact mechanics in a cadaveric knee. This objective can only be reasonably achieved if the biomechanical measuring tools show adequate reliability. Therefore, the first and main purpose of this study is to evaluate the reliability of the NRRU loading device by measuring the test-retest performance of the loading sequence.

Research Objectives

The greatest challenge when designing a biomechanical testing apparatus is to recreate correct physiological conditions while adequately controlling variables in order to measure the desired outcomes. As such, the objective when designing an apparatus should be to create a device able to provide valid and reliable results, which are also physiologically valid. This entails reproducing an activity of daily living with the most accurate loads available while reducing the artificial constraints of a mechanical device, allowing the three components of joint biomechanics: articular geometry, passive joint restraints and neuromuscular control to dictate the findings and measurements. The main objective of this study will be to develop and establish

the reliability and validity of the knee-testing device, which will be used to reach this goal. More specifically, this study will firstly measure the test-retest reliability of the knee loading apparatus when measuring the contact mechanics of the tibiofemoral joint. Once the UOKS reliability is established, subsequent investigations will study the effects of different muscle force profiles acting at the knee, as well as removal of the anterior cruciate ligament (ACL) on the contact mechanics and kinematics of the tibiofemoral joint.

Relevancy

Investigating and studying the contact mechanics of the tibiofemoral joint is important for the understanding of factors that influence the initiation and progression of knee joint degenerative disease. In fact, exploring the effects of neuromuscular deficiencies on the intra-articular loading and thus the articulating surfaces has not been well established. As mentioned earlier, OA affects mobility and is the leading cause of disability in older individuals (The Arthritis Society). A more complete understanding of the factors that participate in the development of OA will allow professionals to not only implement rehabilitation protocols but also develop prevention measures needed to counteract the adverse effects of the disease. The findings of this study will provide information about the effects of different muscle force profiles on the actual tibiofemoral surface contact mechanics, while providing an experimental protocol using a new knee simulating device. This research project is one step in long term research program aiming to identify neuromuscular control deficits and their effects on joint loading.

Review of literature

The knee

The knee is the largest and the most complex synovial joint in the human body. A synovial joint is an articulation where the bones are joined together by a capsule containing synovial fluid. Combined with the smooth articular cartilage covering the surface of the bones, the synovial fluid creates a low friction environment needed for smooth motion. The knee is composed of three distinguishable joints involving three bones (Hamill and Knutzen, 2009). The largest being the tibiofemoral joint, between the tibia and the femur. Essentially, the medial tibiofemoral compartment of the knee acts as a ball and socket joint while the lateral compartment tends to translate with a combination of rolling and sliding motions. This combination between the medial and lateral compartments translates into an axial rotation of the femur relative to the tibia (Freeman & Pinskerova, 2005). The knee allows for three tibiofemoral rotations: extension and flexion in the sagittal plane, varus-valgus motion in the frontal plane and axial rotation in the transverse plane. In addition to these rotations, knee motion also involves tibiofemoral translations awarding the knee its 6 degrees-of-freedom (DOF). Comprising of anterior-posterior, medio-lateral, and compression-distraction translations, these secondary motions have been studied to gain knowledge into the pathomechanics of knee joints (Benoit et al., 2007). The knee must support the weight of the body and transmit force for locomotion while allowing for a great amount of range of motion (Hamill & Knutzen, 2009). The knee is particularly susceptible to injury because it is situated at the between two long bones thus creating an important type three lever arm and the large mechanical demands of ambulation must rely on soft tissue for support. Added to its extensive use in normal daily activities, the knee is also subject to high compressive and torsional loads often seen in sport activities (Magee, 2002).

The American Association of Orthopedic Surgeons (AAOS) reports that in 2010, there were approximately 10.4 million patient visits to the physician's office because of common knee injuries. In 2008, Clayton et al. (Clayton & Court-Brown, 2008) published a five-year prospective study describing the epidemiology of adult musculoskeletal soft tissue injuries. Among the 2794 patients with ligamentous or tendinous injuries, 37.2% were knee injuries. The most common knee injury identified was an affected meniscus with an incidence of 23.8/100, 000 people, per year. Tibiofemoral joint instability or the inability to properly control the knee's six degrees of motion of the knee has been shown to be implicated in the progression of OA (Collins, Katz, Donnell-Fink, Martin, & Losina, 2013; Herzog & Longino, 2007). Establishing and quantifying the magnitudes of abnormal tibiofemoral motion and thus the neuromuscular control is a sought after objective. This accomplishment would allow the development of evidence-based interventions to modify abnormal joint kinetics and kinematics. Benoit et al. (2007) (Benoit et al., 2007) findings raise uncertainty when trying to establish normative joint kinematic profiles to characterize pathological motion of the healthy knee. Inter-subject variability in knee joint positions during gait suggest that joint excursion instead of joint position may be a more appropriate measure of normal and pathological knee motion. Benoit et al. 2007 (Benoit et al., 2007) state that it is essential to understand normal tibiofemoral motion and properly determine the range of normal tibiofemoral motion of the healthy knee before identifying abnormal or pathological motions associated with clinically relevant questions such as injury mechanisms or factors leading to joint degeneration.

Knee joint loading

Animal studies of altered joint loading have shown that biomechanical factors affect cartilage metabolism. Some of the most dependable animal models of cartilage degeneration and OA involve surgically impairing joint stability, such as transection of the anterior cruciate ligament or removal of the meniscus (T. M. Griffin & Guilak, 2005; Radin et al., 1991). Changes in load distribution across the joints has been demonstrated in experimental osteoarthritis (OA) animal models where intra-articular derangements, such as anterior cruciate ligament (ACL) transections (Hasler, Herzog, Leonard, Stano, & Nguyen, 1998; Herzog, Adams, Matyas, & Brooks, 1993; Herzog et al., 1998) meniscectomies (Kamekura et al., 2005), or repetitive impulse loading (Radin, Swann, Paul, & McGrath, 1982), consistently show evidence of joint degeneration after the experimentation. Furthermore, when introducing an intra-articular derangement to the knee joint of a cat, Herzog's team observed an immediate change in joint loading (Herzog et al., 1993). Patellofemoral surface contact forces decreased by 30 % while muscular strength decreased by 70 %. In a subsequent study (Clark, Herzog, & Leonard, 2002), the same research team noticed that although contact forces increased, average joint contact pressure remained relatively identical. This demonstrates the joints ability to alter its contact mechanics when a change occurs. This is a significant observation made by Herzog and colleagues (1993; 1998; 1998; 1998; 1998; 2000; 2002; 2004; 2005; 2006) through years of research demonstrating that joint degeneration may not be the results of overloading the joint but rather the alteration in the contact mechanics of the articular surfaces resulting from modified loading. Since most of the loading of joints comes from muscular contraction, the role of muscles in controlling joint actions and producing loads has been of major interest in biomechanical research (Herzog 2008, IFMBE Proceedings Vol. 23). Lequesne (1997) (Lequesne, Dang, &

Lane, 1997) uses a quote by L. Sokoloff (1963) in his publication about sport practice and osteoarthritis of the limbs: “Cartilage can survive in a large range of solicitations, but below or beyond, it will suffer.” After a multitude of investigations on cartilage behaviour under loading, in-vivo, in-vitro and epidemiological studies agree that moderate mechanical loading is essential to maintain healthy articular cartilage. This reveals that the biomechanical behaviour of the knee joint will have a direct impact on cartilage health. Li and colleagues (2006) (Li, Moses, Papannagari, Pathare, DeFrate, & Gill, 2006b) found that cartilage was significantly thicker at contact areas than non-contact areas, supporting the fact that articular cartilage loading has an effect on cartilage morphology and homeostasis. The limits of “safe loading” for joints are difficult to identify and has not yet been determined. Increased information on healthy loading of the knee joint will enable the development of more effective evidence based and patient tailored treatments and prevention.

Joint stability and altered joint loading

As described in the previous section, experimental knee loading protocols have been developed to observe the effects of disruptions such as: passive intra-articular structural deficiencies (Brady et al., 2007; Clark, Leonard, Barclay, Matyas, & Herzog, 2005; Clark, Leonard, Barclay, Matyas, & Herzog, 2006; Hasler & Herzog, 1998; Hasler et al., 1998; Ihn et al., 1993; Morimoto, Ferretti, Ekdahl, Smolinski, & Fu, 2009; Paci et al., 2009; Tashman, Collon, Anderson, Kolowich, & Anderst, 2004) or meniscal deficiencies (Alhalki, Hull, & Howell, 2000; Ihn et al., 1993; Lee et al., 2006; Marzo & Gurske-DePerio, 2009; Seo et al., 2009). The contribution of muscle action, which is the main contributor to internal mechanical loading of joints, has only recently been viewed as a potential risk factor for the development articular dysfunction and progression of disease such as OA (Fitzgerald, Piva, & Irrgang, 2004; Herzog &

Longino, 2007; Hortobagyi, Garry, Holbert, & Devita, 2004; Hortobagyi et al., 2005; Lewek, Rudolph, & Snyder-Mackler, 2004; Lewek, Ramsey, Snyder-Mackler, & Rudolph, 2005). Knowing that muscles and joints are functionally interdependent, acting to move the limbs while providing stability and shock absorption (Rehan Youssef, Longino, Seerattan, Leonard, & Herzog, 2009; Shelburne, Torry, & Pandy, 2006), alterations in muscle function will have a direct impact on articular surface loading. In addition, a neuromuscular protective mechanism guides the functional and safe movement of the joint by receiving input from the muscles and ligaments (Hurley, 1999; Youssef et al., 2009). There is evidence to support that abnormal knee joint motion is related to the initiation of osteoarthritis (Andriacchi, Briant, Bevill, & Koo, 2006). Shelburne and colleagues (2006) (Shelburne et al., 2006) state that "the onset and progression of knee osteoarthritis (OA) is often attributed to an injury or pathology that alters load distribution between the medial and lateral compartments of the tibiofemoral joint''. They continue by referring to previous studies (Hurwitz, Sumner, Andriacchi, & Sugar, 1998; Schipplein & Andriacchi, 1991) suggesting that there are two factors that influence the distribution of joint loads between the medial and the lateral compartments: the magnitude of the external varus or valgus moment acting about the knee, and the contributions that the muscles make to support this moment. Lloyd and Buchanan (2001) (Lloyd & Buchanan, 2001) found that the muscles that produce most of the flexion and extension moments at the knee during isometric exercise (i.e., quadriceps, gastrocnemius, and hamstrings) also produce most of the moment needed to resist pure adduction and thus protect against a possibly damaging high varus moment. These three main muscle groups can therefore be considered most important when stabilizing the knee in the single leg stance phase of gait, and in effect limit the adduction moment that promotes varus alignment thus increased medial knee compartment loading and articular surface pressure.

Solomonow et al. (1986) (Solomonow, Baratta, Shoji, & D'Ambrosia, 1986) identified that often forces developed around a joint exceed the capabilities of the viscoelastic tissue of tendons in magnitude and direction. They suggest that in order to maintain equilibrium with agonist muscle action, active muscle forces and torques in opposition to the desired action must be generated by the antagonist muscle, in order to maintain joint stability. Baratta and colleagues (1988) speculated about the potential of altered shear stress areas on the articulating surfaces of the joint with unequal agonist and antagonist activity. They suggested that co-activation favours knee joint stability and equal load distribution over the articulating surface, thus preserving and prolonging cartilage integrity by reducing peak articular surface contact stress. In addition, activation patterns have been found to be modified following muscular training and consequently having effects on knee joint stability. An improper co-activation pattern between the quadriceps and hamstring muscle is speculated to decrease knee stability and consequently increase risks of injury (Baratta et al., 1988; Hirokawa, Solomonow, Luo, Lu, & D'Ambrosia, 1991; MacWilliams, Wilson, Desjardins, Romero, & Chao, 1999).

Knee joint dysfunction has been associated with altered muscle force production in the quadriceps muscles (Hurley, 2003; Rehan Youssef et al., 2009). Herzog (2007) and Youssef (2009) have conducted experimental studies that induced a quadriceps muscle weakness in rabbits. They showed that an alteration in muscle strength induces detrimental changes to the articular cartilage of the concerned joint.

The previously described investigations all suggest or propose that muscle force alterations have an impact on joint mechanics. They continue by adding, that this could have a significant impact on peak pressure distribution measured at the articular surfaces. Herzog and Longino (2007) express that further investigations are needed to show that muscle weakness is an independent risk factor for joint degeneration leading to osteoarthritis. Herzog and Federico

(2006)(Herzog & Federico, 2006) state that "In vivo assessment of joint adaptive and degenerative responses to controlled in vivo loading produced through muscular stimulation is an essential and necessary stage in gaining insight into the clinical problems of onset and progression of joint degeneration. Furthermore, we believe that the precise control of muscle forces (or the loss of muscle control through injury, muscle inhibition, reduced afferent feedback, or aging) is a factor contributing to joint degeneration leading to osteoarthritis." We are in agreement that increased knowledge on the impact of muscle strength alterations on the effects of knee joint contact mechanics is needed.

ACL and knee joint loading

Anterior cruciate ligament (ACL) injuries are one of the most significant knee injuries sustained by athletes in sport (Cerulli et al., 2003; Clayton & Court-Brown, 2008). In the US, it is estimated that ACL injuries occur in 1 out of 1000 people (L. Y. Griffin et al., 2000). ACL injuries have many acute and chronic effects on the quality of life, and are known risk factors for the development of post-traumatic osteoarthritis. Lohmander and colleagues (2004) (Lohmander, Östenberg, Englund, & Roos, 2004) studied a cohort of female soccer players who sustained an ACL injury twelve years earlier. They found that slightly more than 50% of the subjects had radiographic OA in their injured knee, and 80% had a radiographic feature related to OA. Seventy-five percent of the 84 women who answered the quality of life (QOL) questionnaire reported had knee symptoms that substantially affected their knee-related QOL, and 28 subjects (42%) were defined as having symptomatic radiographic knee OA. In young active individuals, ACL reconstruction is often performed to facilitate return to sports and activities that required rapid deceleration and cutting maneuvers (Ryan et al. 2014). Although outcomes of surgery are quite successful in helping individuals return to their respective sports, the outcomes are not

always ideal. Biau and colleagues in 2007 (Biau, Tournoux, Katsahian, Schranz, & Nizard, 2007) showed that only 60% of patients who undergone ACL repair were satisfied with their post-surgical outcome. Degenerative knee-joint surface changes after ACL repair were seen in 82% to 89% of the patients (Fithian et al., 2005; Lohmander et al., 2004). The premier motivation for ACL reconstruction has been to restore normal knee function and thus prevent further damage to the joint. However, the high incidence of osteoarthritis after ACL surgery raises questions about the factors that promote the development of OA. Morimoto (2009) reports that more knowledge is needed about ACL injuries and their effects on tibiofemoral contact area and pressure change (Morimoto 2009). Kessler et al. (2008) (Kessler et al., 2008) recorded a significant lower rate of degenerative changes following only a rehabilitation program compared to ACL reconstruction. Frobell R.B. et al. published two randomized control trials in 2010 (Frobell, Roos, Roos, Ranstam, & Lohmander, 2010) and 2013 (Frobell et al., 2013) reporting that at there are no differences in patient-reported outcomes comparing surgical ACL reconstruction combined with structured rehabilitation and structured rehabilitation alone. Additionally, there is no strong evidence showing that ACL reconstruction will protect the knee from subsequent onset of degenerative changes in the involved knee (Frobell, 2013). Kostogiannis et al. (2007)(Kostogiannis et al., 2007) examined 100 patients with an acute total ACL injury without reconstruction for 15 years. Their study revealed that early modification of activity and neuromuscular rehabilitation resulted in good knee function and an acceptable activity level in the majority of patients.

The results presented by these previously mentioned studies have shown interesting aspects of ACL dysfunction and its impact on tibiofemoral biomechanics. Knowing that restoring ACL integrity with surgery does not result in superior long-term outcomes compared to a

neuromuscular rehabilitation strategy; more information about the role of musculature on tibiofemoral contact mechanics is needed. Additionally, studying the effects of muscle forces and ACL integrity on contact mechanics can provide interesting information on their interactions.

Knee simulators

In 1973, Shaw and Murray (Shaw & Murray, 1973) developed and published the elaboration of a dynamic knee simulator designed to reproduce and measure the kinematics of gait. As listed by Dressler et al. (2010), many devices have since been developed for numerous objectives such as: testing knee ligaments (Bach & Hull, 1994; Hashemi et al., 2007; Whiteside, Kasselt, & Haynes, 1987), evaluating prosthesis performance and wear (Burgess, Kolar, Cunningham, & Unsworth, 1997; Guess & Maletsky, 2005; Maletsky & Hillberry, 2000; Maletsky & Hillberry, 2005) , and to measure dynamic loading from a range a daily activities (DiAngelo & Harrington, 1992; Guess & Maletsky, 2005; Szklar & Ahmed, 1987). The most prevalent utilization of knee simulators is to evaluate the capabilities of the different materials and articular geometries of a wide range of knee prostheses. Whether it is measuring induced stress to ligaments, evaluating the results of reconstructed ligaments, measuring the kinematics of simulated gait or tibiofemoral contact pressures, knee simulators capable of in-vitro testing of the human natural healthy knee are a useful tool in the biomechanics laboratory. Several advantages of using an in-vitro experimental simulation can be described. Firstly, the same cadaver specimen can be altered to create many experimental conditions; limiting inter-specimen variation (Woo, Abramowitch, Kilger, & Liang, 2006). Another advantage is that it is possible to manipulate specific structures while it is impossible to manipulate muscles or ligaments in an in-vivo experimental setting. Although in-vitro experimental models seem to be approaching the closest

physiological representation of an event, simulated load bearing is not well established (Müller, Lo, Wünschel, Obloh, & Wülker, 2009).

Two methods have been used to control dynamic simulators; load controlled and position controlled. However, the loading input and position input data used to drive these models are approaches that are known to have accuracy limitations. The tibiofemoral surface load for the healthy knee is not readily available to drive a dynamic simulation. When using inverse dynamics to measure the knee joint moment, the calculated sum of the forces does not represent the net joint contact force (Buchanan, Lloyd, Manal, & Besier, 2004). The most recent knee simulators used for in-vitro experimentation at the knee joint are: The Kansas Knee Simulator, University of Kansas, Lawrence, KS, USA, which was designed based on the Purdue Knee Simulator: Mark II from Maletsky and Hillberry (2005), the Tuebingen knee simulator developed by Müller and colleagues in 2009, and the MATBA (multi-axis biomechanical testing apparatus) developed by Dressler and Ng in 2010. These sophisticated electronically driven dynamic simulators have many design similarities such as the vertical positioning of the specimen in the device, hip and ankle joint simulation, 6 DOF for physiological simulation of knee joint kinematics, and numerous adjustable variables for experimental adjustability. The main issue with theses recently developed simulators is how the simulation is driven. Whether it is a load driven or kinematic driven simulation, both approaches include limitations to the data that drives the simulation. Load driven simulations rely only on articular geometry and passive constraints such as ligaments fascia and capsule to reproduce motion or contact mechanics, while kinematic driven simulations involve known tibiofemoral kinematic inaccuracies as measured in Benoit et al's paper from 2006. Benoit and colleagues measured inaccuracies when comparing tibiofemoral joint translation measured by tracking skin markers versus intra-cortical bone pins revealing that kinematic analysis using skin markers does not precisely represent the underlying bone

movements. These, in turn, decrease the accuracy of the experimental results found in the investigations using these simulators.

As described earlier, the kinematic profile of the knee is a result of loads applied by the muscles, compressive forces, the geometry of the articular surfaces and external loading. In biomechanical engineering of knee simulators, one of the main objectives is to develop knee simulators that do not directly control the kinematics of the knee. In other words, the kinematic observations during testing are the results of physiological constraints, simulated muscle loading, and weight bearing compressive forces (Maletsky & Hillberry, 2005). Thus when adding a physiologically representative load, the knee is free to react according to its natural constraints provided by the soft tissue of the knee: ligaments, capsule, muscle action, compressive forces, and geometry of articulating surfaces. Contact area and related pressure distributions of the tibiofemoral joint have been studied for many years using different knee simulator designs (Ahmed & Burke, 1983; Ihn et al., 1993; Kettelkamp & Jacobs, 1972; Kurosawa, Fukubayashi, & Nakajima, 1980; Lee et al., 2006; Marzo & Gurske-DePerio, 2009; Morimoto et al., 2009; Riegger-Krugh et al., 1998) The main objectives of the above listed publications was to measure differences in either; contact area, contact pressure, peak pressure, or all three at once. Although these objectives were quite similar, the studies differed greatly with respect to the methodology, which includes a variety of loading mechanisms and measuring technologies. From the above-mentioned publications, it is possible to compare mean contact area, mean contact pressure and peak contact pressure for the tibiofemoral articular surfaces. The motivation behind the previously described biomechanical studies has been the exploration of factors that influence or are influenced by degenerative conditions of the knee joint, commonly OA. To the author's knowledge, the previously listed experimental investigations have, in general, used simulators to observe the biomechanical effects of alterations to the knee joint, however, none have attempted

to measure independently the effects of changes to muscular force profiles on the contact mechanics of the tibiofemoral surfaces. To evaluate these interactions, the effects of the altered knee joint muscle force profiles and its effect on contact mechanics of the articular surface is warranted.

Contact area and pressure measurements

Many different methods have been used to investigate contact area, stresses and pressure in di-arthrodial joints. Such methods enumerated by Harris (1999)(Harris, Morberg, Bruce, & Walsh, 1999) include the use of dye injections; stereo-photogrammetry (Ateshian, 1994); silicone rubber (Kurosawa et al., 1980); 3S technique (Yao & Seedhom, 1991); pressure sensitive film (Ihn et al., 1993; Marzo & Gurske-DePerio, 2009; Riegger-Krugh et al., 1998; Stewart et al., 1995); piezoelectric transducers; micro-indentation transducers (Ahmed & Burke, 1983); computer models(Bartel, Bicknell, & Wright, 1986; Bei & Fregly, 2004), and finite element modeling (Donahue, Hull, Rashid, & Jacobs, 2002). The K-scan system from Tekscan, Inc. (Boston, MA) has many advantages and allows for reliable and reproducible measurements of TKA contact area at different loads and angles throughout knee flexion (Harris et al., 1999). This piezoelectric sensor system can be used more than once and several measurements can be taken during one trial. Moreover, the sensors can be used in physiological environments such as in-vitro investigations or surgical procedures because it can be sterilized (Anderson & Pandy, 2003; Lee et al., 2006; Matsuda, Ishinishi, White, & Whiteside, 1997; Wallace, Harris, Walsh, & Bruce, 1998). Bachus et al. (2006) (Bachus, DeMarco, Judd, Horwitz, & Brodke, 2006), Brimacomb (2009) (Brimacombe, Wilson, Hodgson, Ho, & Anglin, 2009) and Lee (2006) demonstrate that the TekScan system can be confidently used to evaluate area, force and pressure over a wide

range of loads. Wilson et al. (2003) (Wilson, Apreleva, Eichler, & Harrold, 2003) state that the K-scan system is particularly recommended when force distribution measurements are required, when the duration of load application can be controlled, and when the sensor does not have to be cemented to an articular surface. Morimoto (2009) also adds " Although the use of Fuji pressure-sensitive film has been proven to be a reliable technique to measure tibiofemoral joint contact area and pressure, a more advanced method (Tekscan, Boston, MA) has been shown to be more accurate when estimating area and pressure".

In most recent literature measuring contact pressure of biological tissue, the Tekscan sensors have become the most common measuring tool. It is convenient mainly because it is thinner than the Fuji-film sensors, it has the ability to withstand large pressures and be reusable, but most importantly, the Tekscan I-scan system reports in real-time data. This is crucial for the experimental nature of in-vitro loading experimentations.

Methodology

Study Design

There are 3 main purposes to this study. The main objective will be to measure the reliability of an in-vitro experimental protocol using a newly developed University of Ottawa knee joint simulator (UOKS). Additionally, we will examine the effects of changing the simulated muscle forces that cross the knee as well as the removal of the ACL on the tibiofemoral contact mechanics and kinematics. Six muscle groups crossing the knee joint will be simulated in order to represent the force profile of a previously determined event of a functional movement of the knee joint. The chosen event is heel-strike as it has been shown to produce peak knee joint force in the gait cycle (Shelburne et al., 2006). Additionally, a recent study by Taylor and colleagues measured ACL relative strain to be maximal at low flexion angles during normal gait (Taylor, 2012). Therefore, it is reasonable to expect that the most significant change in contact mechanics when comparing pre and post ACL measurements will be revealed during early stance phase versus toe-off for example.

Modifications to the muscle-loading profiles will be studied with respect to six joint contact dependant variables as well as joint rotations and translations in all 3 planes of motion. The six joint contact dependant variables will be: medial compartment contact area (*mcca*), lateral compartment contact area (*lcca*), medial compartment contact pressure (*mccp*), lateral compartment contact pressure (*lccp*), medial compartment peak contact pressure (*mcpcp*), lateral compartment peak contact pressure (*lcpcp*).

Equipment and Data Collection

NRRU loading device

The University of Ottawa loading device was designed in collaboration with the Orthopedics Biomechanics Laboratory (OBL) at the General Hospital in Ottawa. The purpose of the testing fixtures and the testing apparatus are to maintain the cadaver limbs in the proper orientation throughout the quasi-static test phase and apply the appropriate muscle loads and the ground reaction force to the limb to simulate physiological knee contact forces. The first task is to fix both the femur and tibia to fabricated parts that can be loaded by the load frame so that the ground reaction force can be applied. These fabricated parts can be seen in Figure 1 to Figure 3, labeled as “femur fixtures” and “tibia fixtures”. The fixtures are designed to maintain the limbs in the proper orientation throughout the test. In addition, the fixtures simulate the hip and ankle joints of the lower extremity by providing the full 6 DOF. The hip component is designed as a ball and socket joint while the ankle fixture sits in an unconstrained semi-sphere construction. With the limbs oriented correctly, the muscle loads will be applied. This is done through sets of shafts and pulleys. Several shafts are placed around the specimen, which are used to guide the cables along the appropriate muscle lines of actions (provided by Brands 1982 data (BRAND et al., 1982)). Guide pulleys, which can translate along the shafts, are used to ensure the proper lines of actions are simulated. Pulleys are used to apply the quasi-static loads, which are amplified through gearing ratios to the desired muscle loads for each muscle. The weights applied may vary from 1kg to 20 kg depending on the muscle load to be applied.

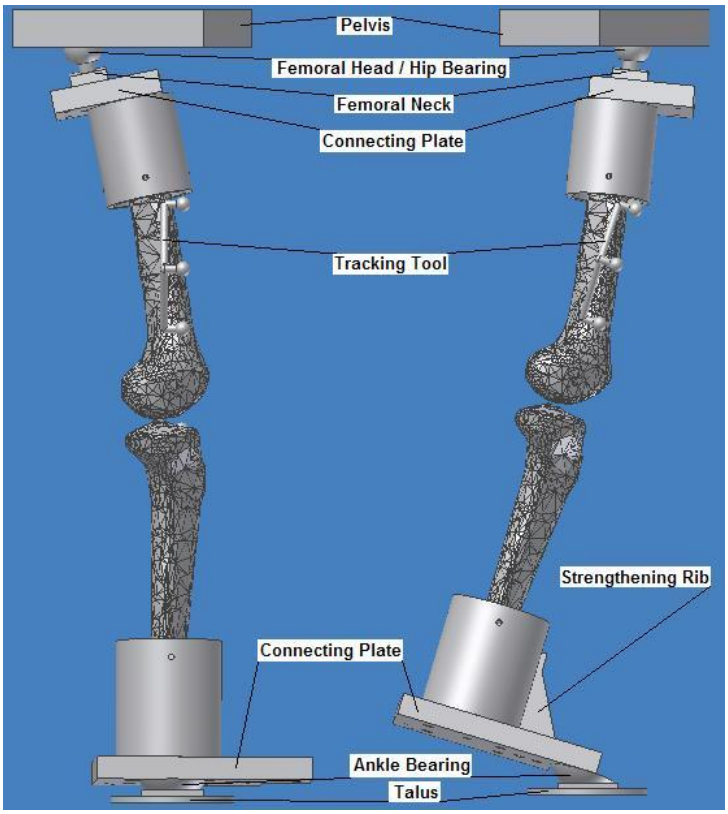

Figure 1. Tibia and femur fixtures assembled to limbs for heel strike and toe off.

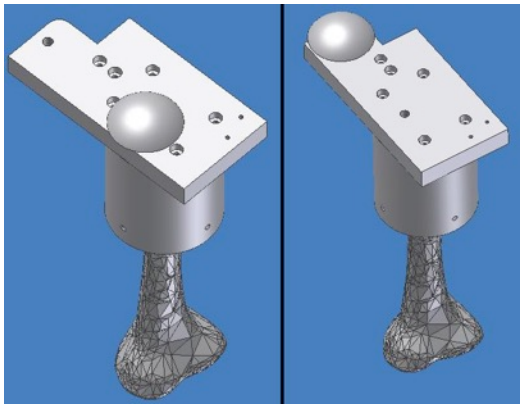

Figure 2. Tibia fixation cup (bottom view) with connecting plate bolted on for heel strike and toe off

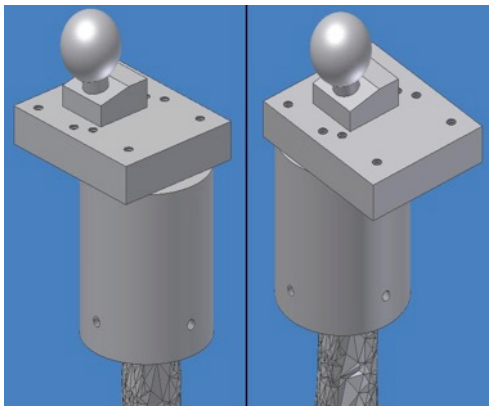

Figure 3. Femur fixtures for heel strike and toe off. Note change of position of alignment plate from frame to frame. Femoral neck block bolts from underside of plate.

Knee specimens and preparation

Six fresh frozen human cadaveric knees will be obtained from the University of Ottawa Faculty of medicine's Division of Clinical & Functional Anatomy, through the Trillium Gift of Life Network. The skin, adipose tissue and muscles are removed carefully while conserving the posterior and lateral joint capsule and the imbedded collateral ligaments. Removing the quadriceps muscles require opening the anterior aspect of the capsule. This is also required to allow access to the joint space for sensor insertion on the tibial plateaus. The patella is released from its attachments to the quadriceps muscles. It is kept on the dissected knee and will be the anchor site for the steel wires that will simulate quadriceps tensioning to reproduce the most physiological patellar tendon lever action. The tibia, fibula and femur are transected at 26 cm from the tibiofemoral articular joint line respectively. They will then be potted into the steel fixtures using a bismuth alloy (Fixtures and apparatus will be discussed in following section). The bismuth alloy is used due to its low melting point of approximately 42^{o}C (so the alloy can be melted in water) and it expands when cooled, creating a strong set for the specimen within the

cast. Once the bismuth has cooled, simulated muscle insertions are reproduced with surgical steel grade plates and screws. To these plates, will be attached the steel aircraft cable needed to reproduce muscle tension as seen in figure 4 below.

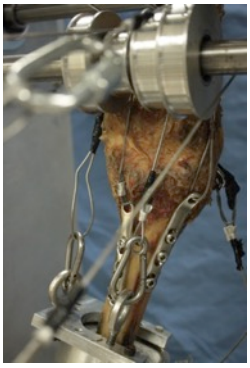

Figure 4. Steel aircraft cables simulating muscles and transmitting muscle force to knee specimen.

Muscle Loading

One way to predict loads at the knee is to measure force plate and kinematic data of a subject moving over the plate. Inverse dynamics are then used to compute the loads at the knee (Hamill and Knutzen, 2009, p 387). Limitations to this method prevent its use for the purposes of the proposed experimentation. Inverse dynamics does not allow individual muscle force to be readily determined from calculated joints moments (Buchanan et al., 2004). However, they have described how to estimate joint moments from EMG signals using a forward dynamics approach. It is a Hill-type model that accounts for force-length and force-velocity relationships of muscle (Buchanan et al. 2005). This model has been able to accurately predict joint moments when compared to measured joint moments. This is of great importance because it accounts for the differences found in an individual's neuromuscular strategy. The EMG driven muscle model

presented by Buchanan et al. (2004) can therefore predict individual muscle loads and joint moments needed for biomechanical studies. The gait kinematics data provides three-dimensional orientation of the femur and tibia throughout the entire gait cycle. The following experimentation will simulate a selected frame of the gait cycle, namely frame 17, which represents heel-strike. The muscle activations collected at this precise time frame are scaled and input into the Hill-type muscle model and muscle forces are computed. Finally, the determined muscle forces are recreated though the pulley system of the U of O knee loading device. Table 8 in Appendix 2 displays the experimental loading conditions and the pulley ratios and required applied loads to the pulley system in order to reach the simulated muscle forces measured by Manal and colleagues (Manal, Gardinier, & Chimera, 2006). The loading conditions chosen for this experimental protocol are mainly based on 2 factors; the fact that this is the first study that will be using the University of Ottawa knee simulator and attempts to recreate conditions of inadequate co-contractions that could alter tibio-femoral contact mechanics. The prior is founded on previous pilot experimentation using embalmed knee specimens and it is not clear how a fresh frozen specimen will react under such loading conditions. On multiple occasions, the embalmed knee fell out of the UOKS under the applied loads and the specimen was damaged. Access to the fresh frozen specimens are limited and they must not be spoiled by compromising the completion of a full data collection because the maximal simulated loads were applied early in the experimental session. It has been therefore decided to scale down the simulated muscle forces for 4 of the 5 loading conditions as described in Appendix 2. As mentioned previously, one of the main goals of this study is to measure the effects of altered muscle loading on tibiofemoral contact mechanics. The second justification for choosing fractions of the maximal muscle loadings is justified by studies such as Suter and colleagues' from 2000 that concluded that knee extensor weakness might be an independent risk factor for development of osteoarthritis. In an attempt to

recreate muscle weakness and simulate a inadequate co-contraction strategy within gait, the present study used fractions of the 100% muscle forces computed by Manal and his colleagues (Manal, Gardinier, & Chimera, 2006) at the University of Delaware, USA. For the UOKS to become a reliable device for in-vitro experimentations, it must demonstrate enough sensitivity to measure changes between loading conditions. For this purpose, the muscle loading profiles seen in Table 9 and Table 10. We expect these muscle imbalances to be important enough to create significant differences in tibio-femoral contact mechanics and kinematics.

Motion capture and analysis

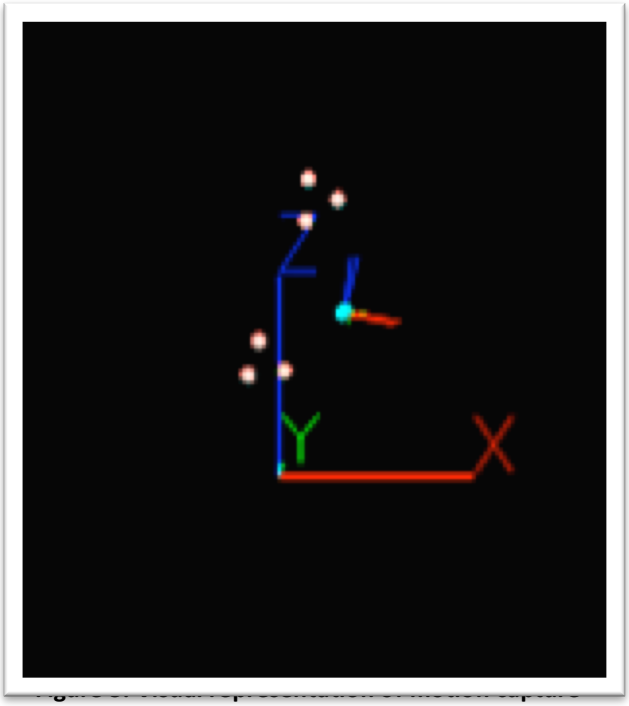

technique using V3D.

A motion capture procedure adapted from Benoit et al. (Effect of skin movement artifact on knee kinematics during gait and cutting motions measured in vivo.2006) was used to measure the relative motion of the femoral and tibia segments. Two reflective marker instruments (comprised of 3-markers each) are attached to the femur and tibia fixtures with intra-cortical bone-pins. A 2010 review by Peters and al. (Peters, Galna, Sangeux, Morris, & Baker, 2010) reported that some limitations to bone-pin use in kinematic measurements have been suggested. Mainly, the bone-pin bending and antalgic gait patterns. These limitations to accurate kinematic measurements relate to in-vivo studies where subjects must walk with intra-cortical bone-pins surgically attached to the femur and shank. The following study is an in-vitro experimentation that only allows very small tibio-femoral translations with a fixed flexion-extension knee angle. We argue that the limitations discussed above will not have an effect on the kinematic measurements from this study. 5 infrared emitting Vicon Cameras, model MX40, recorded the kinematic data through the Nexus 1.5.1 software. The anatomical reference system must be established by digitizing selected known anatomical landmarks (total=10) in addition to the marker triads attached to their respective segments. A custom-built 6DOF knee model was created using Visual 3D software (C-Motion Inc., USA). Technical coordinate systems were created for the femur and tibia segments

respectively with origins defined as the inter-condylar notch and the tibial eminence. The coordinate system is defined by creating virtual anatomical markers using a digitizing pointer. In-total 10 points will be digitized to create the local coordinate system for specimen segment tracking. These anatomical landmarks are displayed and described in Appendix 4. Appendix 5 describes the model building procedure for the individual specimens.

Tekscan I-Scan sensor

The I-Scan Tekscan 4011 sensors from Tekscan Inc. (South Boston, MA) consist of two thin (0.1 mm), flexible polyester sheets, which have electrically conductive electrodes. These electrodes are arranged in rows and columns creating "sensels". The sensor acts as a variable resistor in an electrical circuit. When the sensor is unloaded, its resistance is very high; when a force is applied to the sensor, the resistance decreases. This output resistance is then converted to a digital value. Conditioning a sensor before calibration and testing is essential in achieving accurate results. It helps to lessen the effects of drift and hysteresis. Conditioning is required for new sensors, and for sensors that have not been used for a length of time. To condition the I-scan sensors, a load approximating 110% of the test load will be placed on the sensor. The sensor will be allowed to stabilize, and then removed from loading. Because the interface between the sensor and the test subject material should be the same during conditioning as during calibration and actual testing, a 3 mm thin cartilage analog material is used during conditioning and calibration. (see Appendix 6)

Hydraulic Loading unit and load cell

The University of Ottawa Knee Simulator (UOKS) will be combined with a hydraulic loading system called the MTS 858 Mini Bionix® II from MTS Systems Corporation. This computer driven Hydraulic system includes the load unit with crosshead mounted actuator, an MTS silent flo® hydraulic power unit, and the MTS FlexTest GT® digital controller with at least two channels of control (force and displacement), a refrigerated recirculator, a remote station controller and finally the MTS 858 Mini Bionix® II software. This hydraulic loading device was specifically engineered for testing biomechanical constructs such as, bone, joint, and soft tissue studies. More precisely, simulations of biological forces and displacements such as, kinematic studies of the knee joint or wear studies of hip and knee implant materials. The hydraulic loading system's main contribution to the experimental loading protocol is to allow for reproduction of hip and foot inserts of the lower extremity cadaver specimen. Additionally, the hydraulic system will provide the ability to adjust and measure a physiologically representative GRF, with respect to the position and of the individual muscle contribution of the balanced knee specimen.

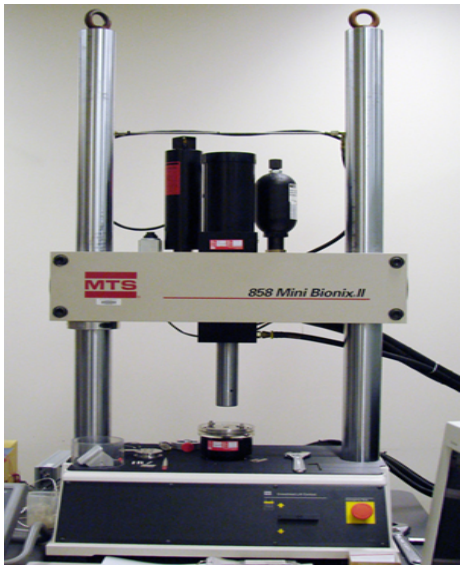

Figure 6. The MTS 858 Mini Bionix II Hydraulic loading system

Experimental protocol summary

The experimental protocol for this research project consists of five main sections. Once a specimen is received from the anatomy laboratory, it must be prepared with careful dissection prior to attaching the muscle insertion sites. Once this is achieved, potting the specimen in its tibial and femoral fixation cups is required. Next, the potted specimen can be installed in the University of Ottawa Oxford Knee loading device, and finally, the loading sequence on the individual muscles is executed. A step-by-step experimental protocol is presented in Appendix 8.

Statistical analysis

Statistical analysis was completed using SPSS (v. 18, IBM, Armonk, USA). We opted for a non-parametric statistical test because assumptions for normality could not be met due to the low sample. Our first objective is to test the repeatability of the measured variables within our experimental protocol.

Test-retest for between-trials, within loading reliability was analyzed using intra-class correlation coefficients (ICC's). An ICC over 0.85 was considered a high correlation coefficient. The Friedman test was used to detect difference between the five muscle loading conditions. The alpha level of significance was considered to be 0, 05 with the independent variables being muscle forces and status of the ACL. The post-hoc analysis following significant differences was computed with a Wilcoxon sign ranked test. The same statistical test was also performed to analyze the effect of removing the ACL. The dependent variables were mean contact area (mm^2), mean contact pressure (MPa), peak contact pressure (MPa) exhibited on the medial and lateral condyles and overall fluctuations in tibial translations (mm) and knee angles (°) during application of loads.

Results

Subject Data

Six fresh frozen lower limb specimens from 2 male donors and 1 female donor were used to collect the following data. Anthropometric data for the 6 lower limbs are found in Table 12 of Appendix 7. Our dissection protocol reveals an intact knee joint with no apparent injury to the cruciate and collateral ligaments. Articular surfaces could only be examined after dissection and therefore could not be a factored in the decision to use a specimen or not. The data used for this study was obtained from 6 lower limb specimens that withheld the applied loads necessary to complete our experimentation. Results and analysis pertinent to the main objective of this research project are presented in the first paper, which can be found in the following section. Additionally, the results obtained in the first analysis gave the opportunity to further the analysis of the obtained data and produce a second article, which had two main objectives; to measure the effects of ACL removal on tibiofemoral contact mechanics as well as the effects of modifying the simulated muscle force that cross the knee joint.

Tibio-femoral joint contact data

Our results have shown that our experimental procedure using the University of Ottawa knee-simulating device can produce very reliable measurements. For repeated trials within the same loading condition, the obtained intra-class correlation coefficients range between 0.926 and 0.99 for all collected dependent variables data (see Appendix 9).

The non-parametric Friedman statistical test complemented by a Kruskal-Wallis post-hoc analysis revealed that the simulated muscle force profiles had a significant effect on tibiofemoral contact area and pressure when the ACL was intact. Significant differences for joint contact dependant variables MCCA, LCCA, MCCP, LCCP, MPCP and LPCP are reported in Table 5 (ACL). In the same table, differences among muscle loads were only evident in MCCP and MPCP once the ACL was removed (Table 5, no ACL). The majority of these differences were in the 50% loading condition, which was significantly different from almost all other loading conditions for all dependent variables.

As seen in Table 5, significant effects on tibiofemoral contact area were observed after ACL transection. Across all five loading conditions, MCCA significantly decreased ($P < 0.05$) from 436.7 mm^2 to 347.7 2 mm^2 after ACL transection while LCCA decreased from 521.8 mm^2 to 405.9 mm^2 after ACL transection. These differences were not seen in mean contact pressure as MCCP and LCCP (2.20 MPa and 2.18 MPa respectively) remained relatively unchanged after ACL removal (MCCP: 2.09 MPa; LCCP: 2.09 MPa). Differences were not seen in peak contact pressure as MPCP (ACL: 6.01 MPa; No ACL: 5.97 MPa) and LPCP (ACL: 7.78 MPa; No ACL: 8.04 MPa) remained stable after ACL transection.

Discussion

The primary aim of this research project was to determine the reliability of the University of Ottawa knee-loading device. With this simulator, we were able to apply five different muscle-loading profiles including simulated weakness on a lower limb to observe their effects on knee joint contact mechanics and kinematics. The experimental protocol developed for this in-vitro study has been developed to allow the applied muscle forces acting on the knee joint to be the only contributors to the production of measured contact mechanics. The UOKS has produced results demonstrating high reliability through very strong ICCs and provides results that concur with the current literature (Riegger-Krugh et al., 1998, Manal K. 2006, Marzo & Gurske-DePerio, 2009) giving an indication that the experimental protocol used with the UOKS can potentially be recognized as a valid in-vitro knee simulation tool (see Appendix 9).

Although tibiofemoral contact area and pressure have been previously studied, caution should be exercised when comparing the raw values of contact mechanic measurements between different in-vitro studies as the sample size for these types of experimentations is usually very small, which makes comparing average values such as contact area more difficult. Moreover, the anthropometric differences between specimens and variability in measurement methods contribute to the inter-study difference. The UOKS and the methods used to obtain data is unique when compared to current in-vitro knee simulators discussed in literature. We are able to load the knee joint specimen with large, physiologically representative muscle forces and GRFs without the need for external constraints. In other words, the observed biomechanics of the knee are produced by physiological factors such as joint geometry, soft tissue constraints and muscle tension in an unconstrained 6DoF environment as would occur in vivo.

As in all in vitro studies, there are limitations with respect to representing in vivo events. We did not represent the impact phase of heel strike despite the effect it can have on in vivo ACL strain (Cerulli, 2003). However, the above study also indicates that the strain remains high after impact and is speculated to be a function of both joint position and muscle loads. As such this compromise did not limit our ability to answer our primary research question, which was the reliability of the device with applied levels of physiological muscle loads.

A second limitation of our experimental procedure is the fact that we do not completely unload the knee specimen between muscle loadings. By doing this, we do allow complete repositioning of the knee joint as it would happen during the swing phase of gait. The knee specimen must be held in place with a constant simulated ground reaction force to stay in the loading simulator. This constant compression of the knee joint can "stabilize" the knee joint and therefore decrease the effect of modifying the muscle loads and by the same mechanism increase the repeatability between multiples trials as reported in tables 13 to 16. This methodological limitation, which is also a loading rate limitation, can also have an impact on the rate-dependent, viscoelastic properties of the soft tissue located in the knee-joint. Even though this is a common limitation among in vitro designs, measuring contact mechanics during a slower rate of loading enables researchers to determine the magnitude and position of the loads being placed on the knee joint. Even though human gait is a dynamic movement, this study focused on quantifying contact forces at a single point in time when muscle forces are at their maximum, rather than tracking the full dynamic movement.

Another limitation was the reduced axial load (500N) applied to the femur through the external actuator. This was a precautionary measure in an attempt to maintain the integrity of the specimens throughout testing. In order to develop the experimental methods described earlier in

the paper, embalmed lower limbs were used to perform pilot studies. During theses trials, whether it was the rapid increase in large simulated muscle loads through the simulator or the decreased structural strength of embalmed tissues versus fresh frozen tissues, the construct failed on multiple occasions. Bones screws used to attach the aircraft cable ripped through the porous bone and the cadaver joint would fall out of the apparatus. Future use of the UOKS will include increasing the axial load to simulate physiological ground reaction forces. Also note that the combined muscle forces applied in the current study are greater than those of past studies, and it is through these large muscle loads that the tibiofemoral joint is most compressed. Even with the reduced axial load our combined internal and external forces results fall in the range of past studies for both contact area (Kurosawa, 1980., Ahmed and Burke, 1983.,Ihn, 1993., Riegger-Krugh, 1998., Portney and Watkins, 2000., Lee, 2006., Marzo and J. Gurske-DePerio, 2009) and pressure (Riegger-Krugh, 1998., Lee, 2006., Manal, 2006. Marzo and J. Gurske-DePerio, 2009). This suggests that past in vitro studies and ours are still underestimating tibiofemoral contact area and pressure. In our case due to the reduced axial load, in others due to their reduced applied muscle forces. By applying greater axial loads to specimens within the UOKS, we expect to predict more physiologically representative joint mechanics than what is currently in the literature.

The aim of the second study was to measure the effect of altering simulated applied muscle load and ACL removal on the contact mechanics of the tibiofemoral joint using a simulator that allows these mechanics to be governed by the soft tissue constraints and applied loads.

Changes were observed between muscle loading profiles for all contact variables in the ACL intact knee specimens; with the ACL removed, changes due to load were only observed for the MCCP and MPCP (see Table 5). Table 6 reveals that for the majority of the reported

dependent variables, the standard deviation, an indication of variability, increased with the ACL removal. We believe that this increase in variability indicates reduced joint stability, which is also supported by the values of Table 4. Although not significant, Table 4,showed increased tibial translations in all but two of the dependent variables once the ACL was removed. It is possible to relate these findings with the degenerative process since small changes in cartilage loading are associated with joint degeneration (Herzog and Longino, 2007). It may be that the small (from a functional point of view) increases in translation and slightly altered rotation angles for the same applied loads, changes that would be undetectable using current gait analysis techniques (Benoit et al, 2007; Andersen et al 2010), are contributing to the degenerative process. Although these findings add support to our observation that the UOKS produces repeatable measurements while demonstrating an adequate amount of sensitivity between loading conditions, we cannot conclude that these changes produce pathological alterations to contact mechanics in keeping with poor co-contractions strategies.

Although, the removal of the ACL can contribute to the above-mentioned findings, ligamentous and muscular components are not the only contributors to joint stability. As described earlier, joint surface morphology is also important contributor to articular stability and posterior tibial slope (PTS) magnitudes, for example, have been described as a variable that can influence tibiofemoral translation and ACL strain (Marouane, 2015). The increased variability in tibiofemoral translation and contact mechanic variable measurements described in the present study after removing the ACL can also be resulting from difference in PTS between specimens. Future studies using the UOKS should record the PTS and include it in the data analysis as a confounding variable. Additionally, the large standard deviation computed for the recorded sagittal flexion-extension angle during data collection reveals that additional modifications to the experimental setup are needed. Optimally, the sagittal flexion angle is identical between

specimens. The simulated muscles forces are the same across all specimen and minimal changes to the joint position will alter the simulated moment at the knee joint. Future experimentation with the UOKS will necessitate identical positioning between specimens prior to data collection.

ACL removal analysis resulted in a consistent decrease in medial and lateral contact area for all load conditions. Hosseini et al (2012) also reported similar results using an in-vivo protocol while measuring tibio-femoral contact area with a dual fluoroscopic and magnetic resonance imaging technique during weight bearing. They reported the average tibial plateau contact area in the intact knee at low flexion angles was just over 500 mm^2 and was significantly reduced to slightly below 400 mm^2 in the ACL deficient state. These results are in agreement with our in vitro results and help validate our research protocol. Even with the observed decrease in contact area, contact pressures remained similar between ACL conditions. Constant pressure measurements following a decrease in contact area corresponds to a decrease in net force measured by the sensor. Because the muscle loading profile and axial load applied to the specimen remained the same across ACL condition, the external forces applied to the knee joint remain the same. The observed decrease in net force between the femur and tibia might be explained by reviewing the complex role of the ACL (Cerulli et al, 2003), which not only restricts anterior tibial translation but applies a portion of its tension axially, effectively increasing joint compression, and is a very plausible explanation for the decreased contact areas following ACL removal.

While contact pressure (MCCP, LCCP, MPCP and LPCP) increased as expected with increasing muscle loads, the contact area did not consistently increase (Table 5). Two possible explanations are apparent to us: the first is that the small kinematic changes shift the centre of pressure on the sensor, unweighting some cells and increasing the pressure on others; the second, and likely in conjunction with the first, is that pressure was distributed to contact areas that were

not covered by the sensor such as the lateral borders on the tibial plateau. As previously discussed, in-vitro studies are accompanied by the non-negligible effect of change in mechanical properties of the soft tissues within the joint due to dehydration. The synovial compartment of an intact knee joint cannot be matched, however, all efforts were made, including using wet compresses and continuous spraying with a saline solution, to maintain fluids around the soft tissues.

In one of there most recent publications, Bergmann and his team state that " loads acting in knee joints must be known for improving joint replacement, surgical procedures, physiotherapy, biomechanical computer simulations, and to advise patients with osteoarthritis or fractures about what activities to avoid" (Bergmann, 2014). Through a series of other studies, the same group has measured knee forces acting in the knee joint with an instrumental tibial tray able to record knee forces and moments. The researchers collected data from these specialized knee prostheses and were able to collect in-vivo measurements, gaining insight into post-operative biomechanics. An important contribution made by in-vivo data is the opportunity for other studies to compare their data and discuss the validity of their approach and their results. Ideally, a cadaver knee equipped with the instrumented tibial tray could be inserted in the UOKS and the collected data could be compared to Bergmann and his team's data. Similar results would confirm that the UOKS is able to reproduce contact mechanics at the tibiofemoral joint as observed in-vivo during gait. As it stands, the results and analyses from this present study cannot confirm that the UOKS produces valid physiological results, however, given our similar contact areas when compared to Hosseini et al (2012), we are confident that our in-vitro simulation was capable of producing results which can be similar to those expected in vivo with changes in muscle load and ACL status.

The University of Ottawa knee simulator development and modifications

The University of Ottawa loading device's defining characteristic is that it uses six simulated muscle lines of action to load the knee joint. For now, it is designed to be a quasi-static knee-loading device that can simulate two important events of gait: heel-strike and toe-off. When designing the simulator, the main purpose was to create a device with which we could measure biomechanically interesting variables without constraining the knee itself. In other words, the objective was to allow for the muscles to dictate the dynamic loading of tibiofemoral joint in combination with the passive constraints of ligamentous tissue and articular geometry.

The loading device was designed in collaboration the Orthopedics Biomechanics Laboratory (OBL) at the General Hospital in Ottawa. A computer-assisted design was created to establish the adequate muscles lines of action that crossing the knee joint. The first modifications to the loading system were to address the accuracy of muscle insertion onto the cadaver specimen. Previously, the patella was removed and the medial and lateral quadriceps simulating cables were inserted directly onto the tibial plateau crossing the knee joint. A rubber insert prevented the cables from hinging onto the femoral condyles. We modified this setup and used a patella bone plate and attached the muscle cables directly onto the patella. We argue that this modification allows the quadriceps muscle force to be distributed in a more physiological manner. The patellar tendon aponeurosis morphology is respected and force transmission to the tibia is achieved onto its native insertion area. This modification was easily applied to the patellar tendon because the patella provided an attachment site for a bone plate and screws. In continuity with our endeavour to provide a more biofidelic application of muscle loads, the optimal solution would be to apply the experimental loads to the native tendons for all the applied loads. This modification to the experimental setup was explored and future use of the UOKS can

consider this approach. As described in Chambers and colleague's paper (Chambers et al, 2015), the respective tendons could be attached to the aircraft cable via a running locked suture, similar to ones used in tendon repairs. This modification to our methodology will retain the specimen's native tendon insertion site and preserve the mechanical properties of force transmission by tendon through the enthesis onto the bone, rather than steel aircraft cable. Tendons possess viscoelastics properties that react to force production from the muscle and in many entheses, the tendons fan out at the attachments sites. This architecture helps distribute the forces applied onto a larger surface area and thus reduces stress to the attachment site. Additionally, the fanning out is accompanied by a reorganization of fibre bundles to provide uniform load transmission or different enthesis loading patterns depending on the joint angle (Zatsiorky and Prilutsky, 2012). Such variables are important to preserve in an experimental setup where physiologic conditions are desired.

Carrying forward with our desire to retain most of the soft tissues around the knee joint, collateral ligaments were kept intact. This required that we keep the fibula, which was discarded with previous pilot testing. To maintain the LCL, the fibula was rigidly inserted into the metal tibia fixtures. This setup also allows for the fibula to share some of the axial force load from the experimental procedure.

Another advantage of retaining ligaments is there interaction with the menisci. The deep fibers of the MCL will stabilize the medial meniscus onto the tibial surface. During the knee joint dissection, care is taken to retain the transvers knee ligaments that secure the menisci to the tibial plateau as well as the menisco-femoral ligament that joins the medio-posterior aspect of the lateral meniscus to medial aspect of the medial femoral condyle. The integrity of these ligaments is important because the tibiofemoral surface pressure measured will be modified if the menisci do not remain in position on the tibial plateau.

One of the main concerns when preparing the specimen for the loading sequence is the adequate placement of the TekScan sensor in the knee joint. We have developed an efficient technique to insert the sensor while keeping the most soft- tissue around the joint as possible and using the native patella as the attachment for the simulated quadriceps muscle force. Our intent was to provide the knee specimen the most physiological simulated muscle insertion as possible. When the knee is loaded the patella is resting in its original inter-condylar groove and access to the joint is relatively impossible. With increased access to the knee joint, some protocol steps could potentially become much simpler and allow for a more efficient and less time consuming experimentation. Additionally, there have been cases where the patella could not hold the applied loads. The surgical screws used to hold "T" shaped patellar bone plate ripped through the patella as seen in the picture above. This did happen on more than one occasion and usually was anticipated because of the pre-testing condition of the knee specimen being osteo-arthritic and more porous than the successful specimens. Two solutions are possible to this problem. Either the specimen will be chosen with radiographic evidence of sufficient bone density and integrity, or a return to an artificial patella and the muscle-simulating aircraft cable is directly screwed into the tibial tuberosity. The latter option would allow for direct intra-articular visualization. This has four foreseeable advantages in addition to the previously described patellar failing. Firstly, when the first half of the loading conditions is completed and the ACL must be removed, it could be done without removing muscle attachments. This reduces specimen manipulation at the mid-point of the experimentation, which can potentially affect data measurements. Secondly, this change would give access to the sensors while they are in the knee joint. Although, it could be difficult to adjust the sensor once it is glued in place, some manipulation could be used to readjust the sensor if some undesired movement is observed. Thirdly, this modification would allow for easier digitization of intra-articular landmarks used in building the model for kinematic

analysis. Lastly, individual specimen difference in patellar size and length of patellar tendon after dissection can modify the position of the knee in the knee simulator. By returning to the original quadriceps muscle attachments protocol, the standardized position is more easily repeated.

Conclusions

The primary aim of this study was to verify the reliability of a newly developed in-vitro knee simulator, and also to discuss the validity of the approach by comparing it to previous work. Our simulator produces very reliable measurements when analyzing the repeatability of contact mechanics and kinematics within individual loading conditions. Our data also falls within the range of similar studies (Table 11), although we have created an experimental protocol that approaches a more physiologically representative simulation. This is achieved by applying more physiological levels of muscle force and the ability to reliably measure 6DoF tibiofemoral kinematics dictated by those applied forces. The results obtained from the first study has determined that the UOKS can be used to measured in-vitro tibiofemoral contact mechanics after altering independent variables such as levels of muscles force, axial load and ACL integrity. After ACL removal, further experimentation has shown changes in contact mechanics and alterations in soft tissue loading that could reasonably be associated with the degenerative process were recorded. Most interestingly, the latest study has shown an increase in variance of the dependent variables after ACL transection, indicating a clinically significant link between instability and these mechanical variables.

Thesis articles

Introduction

Article 1

In-vitro experimentations hold great advantages and are essential to approximate knowledge obtained from ex-vivo and in-vivo designs, which are not always possible. Before analyzing collected in-vitro data, it is necessary to establish the reliability, sensitivity and validity of the experimental protocol and materials used. The following article describes the experimental protocol when using the UOKS for measuring knee contact mechanics which include contact area, contact pressures, center of force displacement and kinematics.

Article 2

The UOKS 's main advantage is its ability to allow muscle forces and articular geometry to be the only dictators of tibio-femoral contact mechanics when an external load is applied to simulate an event of gait. A previously conducted analysis from the data obtained in the present research project has established the reliability and sensitivity of the UOKS. These results provide support for an investigation into the effects of ACL removal and muscle loading conditions on knee joint contact mechanics and kinematics. To our knowledge, the following article is the first in-vitro knee-simulating project to combine ACL removal and multiple muscle-loading conditions to measure changes in tibio-femoral contact mechanics and kinematics.

Article 1:

Tibiofemoral joint contact mechanics measured with a novel muscle load-driven in vitro loading device

Tibiofemoral joint contact mechanics measured with a novel muscle load-driven in vitro loading device

Gauthier, Paul
School of Human Kinetics, University of Ottawa, Canada

Smale, K. Brent
School of Human Kinetics, University of Ottawa, Canada

Speirs, Andrew
Mechanical and Aerospace Engineering, Carleton University, Canada

Dervin, Geoffrey
Department of Surgery, University of Ottawa, Canada
The Ottawa Hospital – General Campus

Manal, Kurt
Department of Mechanical Engineering, University of Delaware, USA

Benoit, Daniel L.[1]
School of Human Kinetics, University of Ottawa, Canada
School of Rehabilitation Sciences, University of Ottawa, Canada
Ottawa-Carleton Institute for Biomedical Engineering

ABSTRACT

Many in vitro knee-loading devices currently exist but none are proficient in measuring tibiofemoral joint contact mechanics caused by physiologically accurate muscle and ground reaction forces. The objective of this study was to describe the University of Ottawa Knee Simulator (UOKS) and evaluate the reliability of tibiofemoral joint contact measurements. With the ACL intact, very high reliability in contact area and pressures among loading conditions were observed as the Intra-class correlation coefficients (ICC) ranged from 0.932 to 0.99. After ACL transection, reliability remained very high as ICCs

[1] Corresponding Author

ranged from 0.926 to 0.99. In summary, the UOKS has demonstrated high reliability within repeated measures and provides valid results that concur with the current literature.

INTRODUCTION

Many knee simulators have been developed for biomechanical studies [1] however we have not identified a device that allows the tibiofemoral joint to move completely unconstrained with six degrees of freedom as the result of applied internal (muscles, body mass) and external (ground reaction) forces. This presents a gap in the literature if the purpose of the in vitro simulator is to provide biofidelic representation of joint loading, in particular since in vivo muscle forces are the only dynamic regulator of joint laxity, and thus a regulator of joint kinematics and kinetics.

Early in vitro work of Markolf et al. [2, 3] focused on joint kinematics and stiffness when compressive loads were applied. This work was expanded upon when Riegger-Krugh et al. [4] measured contact area and pressure under compressive forces after tibial osteotomies, but all three of these studies neglected to include any form of muscle forces. Kinematic-driven simulators have been produced by many research groups to test knee translations and rotations through a range of joint angles, however these typically apply muscle forces that are only a fraction of those that actually occur physiologically [5-7] and many of these neglect the effect that a compressive axial force has on the joint [8, 9]. Since the distinct advantage of in vitro procedures is the ability to manipulate in vivo events, a study that applies large compressive, shear and muscle forces while allowing the bones to move as a function of these loads is necessary, as the larger loads will better resemble contact mechanics and stiffness observed in in vivo situations. Furthermore, since the interest of our research group is to understand the relationship between neuromuscular control and joint stability in healthy and pathological populations, in particular those who demonstrate the combination of reduced knee

stability and altered neuromuscular control such as anterior cruciate ligament injured or osteoarthritic populations, we required a system that allowed the joint mechanics to be dictated in vitro by similar conditions to in vivo.

The University of Ottawa Knee Simulator (UOKS) was designed in collaboration with the Orthopaedics Biomechanics Laboratory at the Ottawa General Hospital with the objective of developing a device that was minimally constrained and sensitive enough to simulate joint loading patterns when subjected to large physiological forces. This means that the device allows for the muscles to dictate the mechanics of the tibiofemoral joint in combination with the passive constraints of ligamentous tissue, articular geometry and applied external (ground reaction force – GRF) loads. The aim of this study was to determine the reliability of the UOKS and discuss the validity of our approach.

METHODS

In vitro preparation: Six fresh-frozen leg specimens were obtained from the University of Ottawa, Faculty of Medicine's Division of Clinical and Functional Anatomy. Both lower limbs of three donors aged 66, 65 and 67 were used for this study. The use of human cadavers in the UOKS was approved by the Ottawa Hospital Research Ethics Board as protocol #20130119-01H. All skin, adipose and muscle tissue was removed while all ligaments were left intact. The anterior capsule was opened when the quadriceps were removed from their patellar attachment. Incisions to the medial and lateral side of the patella and patellar tendon were conducted to expose the tibiofemoral joint and allow for the placement of the pressure sensor (K-Scan 4011, Tekscan, Boston, USA). The patella was left intact, as this was the anchor point for the medial and lateral quadriceps insertions. The tibia, fibula, and femur were then cut 26 cm measured from

the centre of the articulating tibiofemoral joint and both ends of the specimen potted into steel fixtures with the use of bismuth alloy (Figure 7). This method ensures that the bones are securely placed within the fixtures and will not shift during testing.

The potted femur, tibia and fibula are attached to fixtures that are adjustable to simulate the different portions of the stance phase. These fixtures simulate the hip and ankle joints and are responsible for maintaining the position of the knee with six degrees of freedom throughout testing. The simulated hip joint is designed as a ball and socket joint with the ball being located on the femoral fixture and the socket on the MTS loading device (Model 858 Mini Bionix, MTS, Eden Prairie, USA). When the ball on the femoral fixture is inserted into the socket, there is approximately 50% coverage. The simulated ankle joint is comprised of a semi-sphere attached to the tibial fixture, which rests unconstrained on a concave platform located on the MTS load cell. Note that at this stage the in-vitro specimen is not fixed in place and, without muscle loads, must be held in the testing device externally since it is the application of muscle loads and simulated body weight that will, in fact, produce and maintain the test position. One marker triad was drilled into the femoral pot fixture with bone pins, while a second into the tibial fixture (Figure 7). All kinematic data was collected at 100 Hz and analyzed with a custom knee joint model through Visual 3D software (v.4, C-Motion, Germantown, USA). The data reported represent the joint positions during testing with the muscle loads applied. A pointer fastened with three markers was used to identify the bony landmarks and segment origins of the tibia and femur necessary to reconstruct the anatomical coordinate systems and report bone positions based on the system described by Benoit et al [10].

After potting, the six simulated muscles insertions (medial quadriceps, hamstrings, gastrocnemius, and lateral quadriceps, hamstrings, gastrocnemius) were added to the knee so that they act along physiologically correct lines of action. Once the limb is loaded to the correct orientation as described by the musculoskeletal model, muscle loads were then applied by six sets of hanging weights to produce the desired force. The weights pull on steel cables that are attached to their respective insertion points and travel through simple pulley systems to ensure that the forces are being applied to appropriate lines of action [11]. During pilot studies, it was found that the hamstring bone plates and screws could not withstand the applied tensile forces so to solve this issue, a plumber's clamp was wrapped around the bone plates and tibia so that the load applied through the simulated hamstrings was dispersed throughout the attachment, which eliminated the bone plate and screws failure.

In order to access the ACL without the need to unload or dismantle the system, a fine serrated wire (1.5 mm diameter) was carefully looped around the (ACL), folded upwards and taped to the femoral shaft so as not to interfere with testing. After the healthy loading conditions, this wire was used to cut the ACL by gently grasping each end and sawing through the ligament. The wire is removed and testing can then continue; pilot testing and inspection of the joint confirmed that only the ACL was affected by this procedure with no damage occurring to the posterior cruciate ligament or menisci. Note that throughout the entire preparation and testing procedure, the knee joint specimen is consistently sprayed with saline solution to maintain moisture levels within the soft tissues.

Estimation of muscle force: A forward-inverse dynamics Hill-type model [12] was then applied to the gait of a 68 year old male with a height and weight of 1.76 m and 77.1 kg to predict the individual muscle forces that act upon the knee joint [13]. The resulting forces that correspond to the 100% force values of the six simulated muscle groups are displayed in Table 1.

In vitro protocol: The muscle loading sequence was randomized for the exception of the last three, which were the 100% all muscle trials. This step was taken to reduce the chance of damaging the knee with the applied muscle loads. The five muscle force profiles (derived from the in vivo activation profiles) were applied to each specimen three times when the ACL was intact as well as transected, cumulating to a total of 30 trials. The five loading conditions were 50%, 75%, and 100% of max force of all muscles, quadriceps weakness (75% of hamstrings and gastrocnemii forces and 50% of maximum quadriceps force), and finally hamstring weakness (75% quadriceps and gastrocnemii forces and 50% of maximum hamstrings force). All muscles were incrementally loaded or unloaded so that a balance among agonists and antagonists was maintained. Due to the unconstrained nature of the setup, if individual muscle groups were loaded to their maximums all at once, an imbalance would occur, forcing the knee cadaver into unwanted and possibly damaging positions. Once the appropriate load had been applied to each of the six muscle insertions, a 500 N compressive load that represented the ground reaction force was applied to the specimen by the loading device. Since the peak muscle forces were estimated to occur at approximately 25% of the stance phase, which still is double support, 500 N was used to represent slightly over half the body weight of a male participant.

Statistical analysis: Statistical analysis was completed using SPSS (v. 18, IBM, Armonk, USA). Test-retest for between-trials reliability was analyzed using two-way, mixed, intra-class correlation coefficients (ICC's). An ICC over 0.85 was considered a high correlation coefficient and corresponds to a high level of reliability [14]. The dependent variables were mean contact area (mm^2), mean contact pressure (MPa), peak contact pressure (MPa) exhibited on the medial and lateral condyles respectively, and overall fluctuations in tibial translations (mm) and knee angles (°) during application of loads.

RESULTS

The intra-class coefficients for tibiofemoral kinematics, contact area and pressure were all very high (0.926 – 0.99) indicating a high reliability when collecting repeated measures for our dependent variables. During repeated trials of each muscle loading condition with the ACL intact, ICCs ranged from 0.932 – 0.99, again indicating a high degree of reliability among repeated muscle loads. Once the ACL was removed, computed ICCs ranged from 0.926 to 0.99. These high values show that the UOKS is a very reliable apparatus when testing the effects muscle forces have on tibiofemoral joint contact mechanics. Table 2 displays the averaged tibiofemoral contact and kinematic data. The 95% confidence interval (CI) indicated in Table 2 provides the margin of error to be expected using the device. As a conservative estimate the highest value of the grouped dependent variable (mm^2, MPa, degrees or mm respectively) are used to describe this error.

DISCUSSION

The methods used for this in-vitro research project have been developed to allow for the knee specimen and its applied muscle forces to be the only contributors to the production of measured contact mechanics. The UOKS has demonstrated high reliability through very strong ICCs and provides results that concur with the current literature [4, 13-20], giving an indication that the experimental protocol used with the UOKS can potentially be recognized as a valid in-vitro knee simulation tool.

Although contact area and pressure are common variables in in vitro studies, caution should be exercised when comparing the raw values of contact mechanic measurements between even slightly different in-vitro studies as the sample size for these types of experimentations is typically very small, ranging from four to ten specimens, limiting the ability to compare average values such as contact area for example. Furthermore, the anthropometric differences between specimens and variability in measurement methods contribute to the inter-study difference. This is particularly the case here since we allow the joint kinematics to be determined by the muscle and GRF loads, as is the case in vivo, rather than be predetermined by the test jig.

The UOKS holds distinct characteristics with respect to the current in vitro knee loading devices being reported in the literature. In addition to the knee joint being kinematically unconstrained except by the applied loads, the simulator is capable of applying the large physiological muscle, shear and ground reaction forces that occur naturally in instances of human movement such as heel strike during gait. Past loading devices have not had been capable of simulating these large muscle and ground reaction forces in combination while recording pressure or contact mechanics within the

tibiofemoral joint and allowing the joint to respond with six degrees of freedom as would occur in vivo.

An in vitro device must demonstrate sensitivity and reliability in addition to a physiologically relevant application. The UOKS was sensitive enough to detect meaningful changes in joint mechanics with the removal of the ACL. The device also produced repeatable results for all collected data as demonstrated by high ICC values.

As in all in vitro studies, there are limitations with respect to representing in vivo events. We did not represent the impact phase of heel strike despite the effect it can have on in vivo ACL strain [23]. However, the above study also indicates that the strain remains high after impact and is speculated to be a function of both joint position and muscle loads. As such this compromise did not limit our ability to answer our primary research question, which was the reliability of the device with applied levels of physiological muscle loads. A second limitation was the reduced axial load (500N) applied to the femur through the external actuator. This was a precautionary measure in an attempt to maintain the integrity of the specimens throughout testing. Future use of the UOKS will include increasing the axial load to simulate physiological ground reaction forces. Also note that the combined muscle forces applied in the current study are greater than those of past studies, and it is through these large muscle loads that the tibiofemoral joint is most compressed. Even with the reduced axial load our combined internal and external forces results fall in the range of past studies for both contact area [4, 14–16, 18–20] and pressure [4, 13, 19, 20]. This suggests that past in vitro studies and ours are still underestimating tibiofemoral contact area and pressure. In our case due to the reduced axial load, in others due to their reduced applied muscle forces. By applying greater axial

loads to specimens within the UOKS, we expect to predict more physiologically representative joint mechanics than what is currently in the literature.

Another limitation is that the loading rate of our device cannot take into account the rate-dependent, viscoelastic properties of the soft tissue located in the knee-joint. Even though this is a common limitation among many in vitro designs, measuring contact mechanics during a slower rate of loading still enables researchers to determine the magnitude and position of the loads being placed on the knee joint. These data can help detect altered loading patterns and perhaps identify the patterns that may put the knee at risk of soft tissue degradation. Furthermore, this study focussed on quantifying contact forces at a single point in time rather than tracking the full dynamic movement. Even though human gait is a dynamic movement, this was done as a first step to control as confounding variables such as the rate and history of loading. By doing so, we are able to take a brief 'snapshot' of what tibiofemoral joint loading when muscle forces are at their maximum.

CONCLUSION

The primary aim of this study was to verify the reliability of a novel in vitro knee simulator and discuss the validity of the approach in light of the limitations of in vitro research. Our simulator provides very reliable measurements when analyzing the repeated measures within individual loading conditions. The margins of error are small using the device and well below the expected clinically significant level for the related dependent variable. Our data also falls within the range of similar studies, although we provide a platform that allows for more physiological levels of muscle force and the ability to reliably measure 6DoF tibiofemoral kinematics dictated by those applied forces.

The results from this study give an indication that the experimental protocol used with the UOKS can potentially be recognized as a valid in-vitro knee simulation tool for further analysis of tibiofemoral contact mechanics and kinematics during loading conditions which alter independent variables such as ACL status, levels of muscle forces and axial load. We will use this platform to evaluate the mechanics of the joint when altering these independent variables.

ACKNOWLEDGMENT

The authors would like to thank Hakim Louati of the Orthopedics and Biomechanics Lab as well as all donors and their family members who without their generosity, this and future in vitro studies could not be completed.

FUNDING

This study was funded by the Natural Sciences and Engineering Research Council (NSERC) of Canada and the Canadian Foundations for Innovation.

REFERENCES

[1] J. L. Dressler, R. T. Ng, A. Amirfazli, and J. P. Carey, "Development and evaluation of a multi-axis biomechanical testing apparatus for knee," *Int. J. Exp. Comput. Biomech.*, vol. 1, no. 3, pp. 271–295, Jan. 2010.

[2] K. L. Markolf, W. L. Bargar, S. C. Shoemaker, and H. C. Amstutz, "The role of joint load in knee stability," *J. Bone Jt. SurgeryAmerican Vol.*, vol. 63, no. 4, pp. 570–585, Apr. 1981.

[3] K. L. Markolf, J. S. Mensch, and H. C. Amstutz, "Stiffness and laxity of the knee–the contributions of the supporting structures. A quantitative in vitro study," *J. Bone Jt. SurgeryAmerican Vol.*, vol. 58, no. 5, pp. 583–594, Jul. 1976.

[4] C. Riegger-Krugh, T. N. Gerhart, W. R. Powers, and W. C. Hayes, "Tibiofemoral contact pressures in degenerative joint disease," *Clin. Orthop.*, vol. (348), no. 348, pp. 233–245, Mar. 1998.

[5] Y. K. Oh, J. L. Kreinbrink, J. A. Ashton-Miller, and E. M. Wojtys, "Effect of ACL transection on internal tibial rotation in an in vitro simulated pivot landing," *J. Bone Jt. SurgeryAmerican Vol.*, vol. 93, no. 4, pp. 372–380, Feb. 2011.

[6] P. A. Torzilli, X. Deng, and R. F. Warren, "The effect of joint-compressive load and quadriceps muscle force on knee motion in the intact and anterior cruciate ligament-sectioned knee," *Am. J. Sports Med.*, vol. 22, no. 1, pp. 105–112, Feb. 1994.

[7] T. J. Withrow, L. J. Huston, E. M. Wojtys, and J. A. Ashton-Miller, "The relationship between quadriceps muscle force, knee flexion, and anterior cruciate ligament strain in an in vitro simulated jump landing," *Am. J. Sports Med.*, vol. 34, no. 2, pp. 269–274, Feb. 2006.

[8] O. Müller, J. Lo, M. Wünschel, C. Obloh, and N. Wülker, "Simulation of force loaded knee movement in a newly developed in vitro knee simulator," *Biomed. Tech. (Berl)*, vol. 54, no. 3, pp. 142–149, Jun. 2009.

[9] J. D. Yoo, R. Papannagari, S. E. Park, L. E. DeFrate, T. J. Gill, and G. Li, "The effect of anterior cruciate ligament reconstruction on knee joint kinematics under simulated muscle loads," *Am. J. Sports Med.*, vol. 33, no. 2, pp. 240–246, Feb. 2005.

[10] D. L. Benoit, D. K. Ramsey, M. Lamontagne, L. Xu, P. Wretenberg, and P. Renstrom, "Effect of skin movement artifact on knee kinematics during gait and cutting motions measured in vivo," *Gait Posture*, vol. 24, no. 2, pp. 152–164, Oct. 2006.

[11] R. A. Brand, R. D. Crowninshield, C. E. Wittstock, D. R. Pedersen, C. R. Clark, and F. M. van Krieken, "A model of lower extremity muscular anatomy," *J. Biomech. Eng.*, vol. 104, no. 4, pp. 304–310, Nov. 1982.

[12] T. S. Buchanan, D. G. Lloyd, K. Manal, and T. F. Besier, "Estimation of muscle forces and joint moments using a forward-inverse dynamics model," *Med. Sci. Sports Exerc.*, vol. 37, no. 11, pp. 1911–1916, Nov. 2005.

[13] K. Manal, J. Gardinier, and N. Chimera, "What are we missing when using inverse dynamics?," in *Proceedings of the American Society of Biomechanics*, 2006, vol. 30.

[14] L. G. Portney and M. P. Watkins, *Foundations of Clinical Research: Applications to Practice*. Prentice Hall, 2000.

[15] A. M. Ahmed and D. L. Burke, "In-Vitro of Measurement of Static Pressure Distribution in Synovial Joints—Part I: Tibial Surface of the Knee," *J. Biomech. Eng.*, vol. 105, no. 3, pp. 216–225, Aug. 1983.

[16] J. C. Ihn, S. J. Kim, and I. H. Park, “In vitro study of contact area and pressure distribution in the human knee after partial and total meniscectomy,” *Int. Orthop.*, vol. 17, no. 4, pp. 214–218, Aug. 1993.
[17] D. B. Kettelkamp and A. W. Jacobs, “Tibiofemoral Contact Area-Determination and Implications,” *J. Bone Jt. Surg.*, vol. 54, no. 2, pp. 349–356, Mar. 1972.
[18] H. Kurosawa, T. Fukubayashi, and H. Nakajima, “Load-bearing mode of the knee joint: physical behavior of the knee joint with or without menisci,” *Clin. Orthop.*, no. 149, pp. 283–290, Jun. 1980.
[19] S. J. Lee, K. J. Aadalen, P. Malaviya, E. P. Lorenz, J. K. Hayden, J. Farr, R. W. Kang, and B. J. Cole, “Tibiofemoral Contact Mechanics After Serial Medial Meniscectomies in the Human Cadaveric Knee,” *Am. J. Sports Med.*, vol. 34, no. 8, pp. 1334–1344, Aug. 2006.
[20] J. M. Marzo and J. Gurske-DePerio, “Effects of Medial Meniscus Posterior Horn Avulsion and Repair on Tibiofemoral Contact Area and Peak Contact Pressure With Clinical Implications,” *Am. J. Sports Med.*, vol. 37, no. 1, pp. 124–129, Jan. 2009.
[21] Y. Morimoto, M. Ferretti, M. Ekdahl, P. Smolinski, and F. H. Fu, “Tibiofemoral joint contact area and pressure after single- and double-bundle anterior cruciate ligament reconstruction,” *Arthrosc. J. Arthrosc. Relat. Surg. Off. Publ. Arthrosc. Assoc. N. Am. Int. Arthrosc. Assoc.*, vol. 25, no. 1, pp. 62–69, Jan. 2009.
[22] S.-Y. Poh, K.-S. A. Yew, P.-L. K. Wong, S.-B. J. Koh, S.-L. Chia, S. Fook-Chong, and T.-S. Howe, “Role of the anterior intermeniscal ligament in tibiofemoral contact mechanics during axial joint loading,” *The Knee*, vol. 19, no. 2, pp. 135–139, Mar. 2012.
[23] G. Cerulli, D. L. Benoit, M. Lamontagne, A. Caraffa, and A. Liti, “In vivo anterior cruciate ligament strain behaviour during a rapid deceleration movement: case report,” *Knee Surg. Sports Traumatol. Arthrosc.*, vol. 11, no. 5, pp. 307–311, Sep. 2003.

Figure Captions List

Table Caption List

Table 1. Applied load through hanging weights and their corresponding simulated muscle loads. The hanging weight load for each muscle is magnified by their individual pulley systems to achieve their simulated muscle load.

Table 2. Average tibiofemoral contact data collected from six fresh-frozen knee specimens. Contact area, pressures and peak pressures are displayed for both medial and lateral compartments (Med comp, Lat comp) in the knee. The 95% confidence interval (CI) for the highest value of each dependant measure is noted and represents the margin of error.

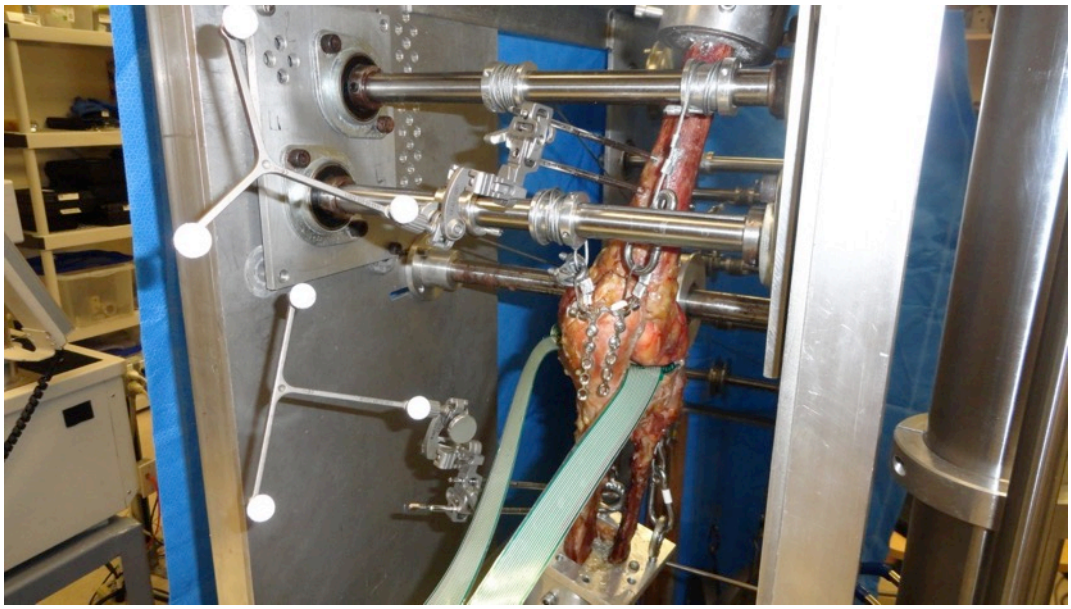

Figure 7

Table 1.

	QUADRICEPS		HAMSTRINGS		GASTROCNEMIUS	
	Medial	Lateral	Medial	Lateral	Medial	Lateral
SIMULATED LOAD (N)	406	1009	258	155	157	69
HANGING WEIGHT (KG)	20.41	40.82	11.34	11.34	4.54	4.54

Table 2

	CONTACT AREA (MM^2)		CONTACT PRESSURE (MPA)		PEAK CONTACT PRESSURE (MPA)		JOINT ANGLES (°)			TRANSLATIONS (MM)		
	Med comp	**Lat comp**	**Med comp**	**Lat comp**	**Med comp**	**Lat comp**	**Flex-Ext**	**Abd-Add**	**Med-Lat rotation**	**Med-Lat**	**A-P**	**Dist-Comp**
ACL	432.23± 3.34	525.54± 3.08	2.12± 0.05	2.04± 0.03	5.68± 0.10	7.22± 0.27	11.70± 5.83	1.18± 1.63	-6.90± 4.28	0.63± 0.62	0.64± 0.39	0.55± 0.27
NO ACL	354.78± 1.32	406.96± 2.16	2.01± 0.05	2.05± 0.05	5.79± 0.08	7.81± 0.22	13.31± 5.46	2.36± 1.39	-11.40± 6.92	0.73± 0.70	0.72± 0.49	0.65± 0.35
95% CI	± 2.67 mm^2		± 0.22 MPa		±0.22 MPa^2		±4.37 degrees			±0.56mm		

Article 2:

The effect of muscle forces and ACL resection on in vitro knee contact mechanics using a minimally-constrained, 6 DoF preparation.

The effect of muscle forces and ACL resection on in vitro knee contact mechanics using a minimally-constrained, 6 DoF preparation.

Running Title: In vitro knee contact mechanics

Paul Gauthier [1], K. Brent Smale [2], Andrew Speirs[3], Kurt Manal[4],
Geoffrey Dervin[5], Daniel. L. Benoit [1, 2, 6]

[1] School of Rehabilitation Sciences, University of Ottawa, Canada;
[2] School of Human Kinetics, University of Ottawa, Canada,
[3] Carleton University Department of Mechanical Engineering,
[4] Department of Mechanical Engineering, University of Delaware,
[5] Faculty of Medicine, Department of Orthopedics, University of Ottawa, Canada,
[6] Ottawa-Carleton Institute for Biomedical Engineering, Ottawa, Canada

Corresponding Author:
Daniel Benoit

Abstract

Understanding the relationship between muscle loads crossing the knee joint and knee joint mechanics is critical for understanding knee stability and the effects of altered muscle forces on healthy and ACL injured knees. In vitro measurement can be used to elucidate this if the simulation is biofidelic, allowing the physiological levels of applied loads to dictate the tibiofemoral kinematics in all degrees of freedom (DoF). The objective of this study was to describe and apply a device, which allows 6 DoF tibiofemoral motions, is constrained through a simulated hip and ankle joint and accepts high levels of muscle forces from six simulated knee joint muscles. This device was used to quantify the effect of muscle loads and anterior cruciate ligament (ACL) resection on contact mechanics and kinematics of the tibiofemoral joint. Muscle forces were determined from an electromyography-driven musculoskeletal model of a healthy male during gait. Six knee specimens were loaded into the simulator and subjected to 100%, 75% and 50% in vivo muscle forces applied through the 6 simulated muscles, in addition to a quadriceps weakness and a hamstring weakness condition. Tibiofemoral mechanics were measured with all 5 loading conditions before and after ACL transection. In all conditions, muscle forces maintained the knee joint in a stable position resulting in minimal kinematic differences, but altered contact mechanics in both the ACL and non-ACL condition. Removal of the ACL significantly reduced both the medial and lateral contact areas in all loading conditions compared to the ACL intact condition. Small, normally undetectable alterations in joint kinematics resulted in significant alterations to contact mechanics, which can be linked to the degenerative process.

Key Words: ACL, in vitro, tibiofemoral, contact area, contact pressure

Introduction

The biomechanical behaviour of the knee joint will have a direct impact on cartilage health. An injury to the anterior cruciate ligament (ACL) leads to passive laxity and often occurs in combination with injuries to neighboring soft tissue such as the menisci. The majority of those suffering an ACL injury (60-90%) will develop knee joint osteoarthritis (OA) as evidenced by radiological changes just 10-15 years post injury (Lohmander et al, 1994). Using animal models, similar degenerative changes have been provoked after just four weeks of induced quadriceps weakness: Herzog and colleagues (Hasler et al, 1998; Herzog and Suter, 1997; Herzog and Longino, 2003) first hypothesised that reducing the stabilizing integrity of the joint would result in greater forces being transmitted to the articulating surfaces, and thus facilitate degeneration. However, they observed decreases in peak contact forces and pressures despite increasesin contact areas. From a biomechanical point of view what can also be deduced from their findings is that, since small changes in joint kinematics (the relative position of the tibia with respect to the femur) occurred with increased laxity, peak pressure (and thus force) can be reduced despite an increase in area since new surfaces may be interacting. Therefore, they concluded that the onset of OA might not have been the direct result of cartilage overloading but rather an alteration in the contact mechanics resulting from compromised knee stability.

Despite suffering form an ACL tear, most patients treated conservatively can return to an acceptable activity level and knee function up to 15 years post injury as measured by the KOOS (Ageberg and Pettersson, 2007), while still others are able to return to high levels of activity (Lewis 2008; Barenius, 2010). This would indicate that knee joint musculature; even with the moderately reduced capacity observed post injury, can maintain joint integrity during activities of daily living such as gait. Nevertheless, the majority of those injured will develop knee

osteoarthritis (Lohmander et al, 1994), indicating that changes to joint cartilage loading, however minor, may be provoking the degenerative process.

Knee stability arises from the integration of articular geometry, soft tissue restraints, compressive loads from weight bearing and muscle forces (Yoo et al, 2005). Of these, muscles are the only active regulators of knee joint stability and, interestingly, the combined effects of weight bearing and muscle forces have been shown to maintain joint stability as measured by anterior tibial translation even with the elimination of passive tissue restraints (Hsieh et al, 1976). As such, it is reasonable to expect only very small alterations in kinematics with the removal of the ACL under physiological levels of muscle loading.

Currently there are few studies that link individual muscular loads crossing the knee with contact mechanics. The work of Markolf et al. (1976, 1981) focused on joint kinematics and stiffness when compressive loads were applied. This work was expanded upon when Riegger-Krugh et al. (1998) measured contact area and pressure under compressive forces after tibial osteotomies, but all three of these studies neglected to include any form of muscle forces. Kinematic-driven simulators have been developed to evaluate knee translations and rotations through a range of joint angles, however these typically apply muscle forces that are only a fraction of those that actually occur physiologically (Oh et al, 2011; Torzilli et al, 1994; Withrow et al, 2006) and many of these neglect the effect that a compressive axial force has on the joint (Muller et al, 2009; Yoo et al, 2005). A novel in vivo/in vitro dynamic simulator has also recently been developed which simulates the dynamic sagittal plane motion of the knee during jump-landing and provides useful insight into the relationship between knee flexion and ACL strain (Cassidy et al, 2013) however rotations in the frontal and transverse planes are restricted. Since the distinct advantage of in vitro procedures is the ability to manipulate in vivo events, a study that applies large physiological muscle and axial loads while allowing the bones to move in 6

DoF as a function of these loads will better resemble contact mechanics and stiffness observed in vivo. This approach may provide insight into how small alterations in joint kinematics can lead to altered cartilage loading that may provoke degenerative change.

The purpose of this study was therefore to use a novel in vitro knee joint simulator to apply physiological levels of force, as determined by an electromyography-based musculoskeletal model measuring a healthy adult male during gait, to a minimally constrained knee joint which allows the tibia and femur to move with 6 DoF as determined by the applied axial loads and muscle forces in order to evaluate the effects of altering muscle load and ACL transection on in vitro knee joint mechanics. It was hypothesized that the new simulator would provide reliable kinematic contact pressure and area readings within muscle loads. Also, as applied muscle loads increase, it is expected that tibiofemoral contact area and pressure will increase accordingly. Finally, since our device allows us to apply the same physiological levels (very high) of axial and muscle loads between ACL and ACL deficient conditions, it was hypothesized that no differences in contact pressure and area would occur after ACL resection.

Methodology

Six fresh-frozen full leg specimens (intact femur, tibia and fibula) from three donors aged 65-67 with minimal signs of knee joint degeneration or previous knee joint injury were obtained from the *University of Ottawa, Faculty of Medicine, Division of Clinical and Functional Anatomy*. The study was approved by the local hospital research ethics board (protocol #20130119-01H). All skin, adipose and muscle tissue was removed from the leg; the anterior capsule was opened when the quadriceps were removed from their patellar attachment and incisions to the medial and lateral side of the patella and patellar tendon, which exposed the tibiofemoral joint and allowed for the placement of the pressure sensor (K-Scan 4011, Tekscan,

Boston, USA). The sensor was calibrated according to manufacturer specifications using a custom made calibration surface that had a spherical end and concave receiver; sensor data was recorded at 5Hz using Tekscan I-scan 5.83 software. The patella and patellar ligament were left intact for use as the anchor point for the medial and lateral quadriceps insertions. All ligaments were left intact, as was the posterior capsule.

A motion analysis pointer tool with 3 reflective markers was then used to digitise the locations of the hip joint centre, medial and lateral femoral epicondyles, femoral inter-condylar notch, medial and lateral edges of proximal tibia, tibial eminence, mid-point medial-lateral distal tibial condyles using a 5-camera Vicon system (MX40 cameras, Oxford UK) and collected with Nexus 1.5.1 software at 100Hz. The tibia, fibula, and femur were then cut 26 cm above the midline of the articulating tibiofemoral joint and both ends of the specimen were potted into metal fixtures representing the hip (Figure 1a; includes a ceramic ball into metal socket) and ankle (Figure 1b; includes brass ball and socket) with the use of melted bismuth alloy. The fixtures simulate the hip and ankle joints of the lower extremity by providing the full 6 DOF as well as maintain the limbs in the proper orientation throughout the test. With the limbs oriented correctly, the muscle loads were applied through 6 sets of shafts and pulleys (figures 1c to 1e). Several shafts are placed around the specimen, which are used to guide the cables along the appropriate muscle lines of actions (provided by Brands 1982 data (Brand et al., 1982)). Guide pulleys, which can translate along the shafts, are used to ensure the proper lines of actions are simulated. The pulleys are used to apply the quasi-static loads, which are amplified through gearing ratios to the desired muscle loads for each muscle. The weights applied may vary from 1kg to 20 kg depending on the muscle load to be applied. Prior to pouring the alloy into the femur and tibia fixtures, bone pins were drilled into both fixtures allowing the alloy to harden around the inserted bone pins. Once the alloy cooled and hardened, one marker triad was securely

attached onto the femoral bone pins and a second onto the tibial bone pins. The triads and remaining specimen landmarks were then re-digitised with the pointer to provide the anatomical coordinates required to reconstruct the local coordinate systems. A custom 6 DOF lower-limb kinematic-recording and analysis model was created using Visual 3D software (C-Motion Inc., Germantown, USA) with the femoral origin defined as the inter-condylar notch and the tibial origin at the tibial eminence. Using the previously recorded marker locations, the long axis of the femur passed through the hip joint, while the long axis of the tibia passed through the centre of the distal tibia. The data reported represents the joint positions of the tibial origin with respect to the femoral origin during testing as described by Benoit et al (2006).

A thin metal serrated wire of 1.5 mm in diameter was then looped around the ACL and above the PCL, folded upwards and held out of the way. After the ACL-intact loading conditions were conducted, this wire was used to cut the ACL. Its initial placement in the knee joint was carefully monitored to ensure it did not damage other tissue, as confirmed through pilot studies and by visual inspection after the specimen was removed.

The muscle insertions sites of the vastus medialis (VM) and lateralis (VL), biceps femoris (BF), semitendinosus (ST), medial (MG) and lateral (LG) gastrocnemius were identified and small modified fracture plates were screwed in at each location such that an open loop at the end of the plate was located over the insertion site. Due to their high-applied loads and muscle lines of action, the hamstring plates were reinforced with a circular clamp to prevent pullout of the fixation screws. Steel cables were then attached to their respective insertion points and travelled through pulley systems, which adjusted the lines of action of each muscle (Figure 1c) to coincide with their respective musculoskeletal model orientation (Brand et al, 1982). The prepared limb was loaded into the simulator so that the specimen's knee joint angle was equal to that of the in vivo data at the point where combined muscle forces were at a maximum. Once the specimen was

correctly positioned, an arbitrarily chosen 200N axial load was applied to the specimen through the hip attachment by a MTS hydraulic loading device, which was equipped with a 6 DoF load cell (Model 858 Mini Bionix, MTS, Eden Prairie, USA). This 200N was required so that the specimen did not collapse under gravity due to its unconstrained nature. Muscle loads were then applied incrementally via the six, previously mentioned, sets of free weights hanging behind the knee simulator (Figure 1d and e) to produce the desired force and the axial load was manually adjusted to maintain the 200N axial load.

The muscle forces applied to the specimens were derived from a previous in vivo study (Buchanan et al, 2005): briefly, a forward-inverse dynamics electromyography-driven Hill-type model (Buchanan et al, 2004) was applied to the gait of a 68-year-old male with a height and weight of 1.76 m and 77.1 kg to predict the individual muscle forces that act upon the knee joint. The muscle forces recorded were at approximately 25% of the gait cycle were used to simulate the heel-strike/weight acceptance event of gait, resulting in estimated forces of: VM = 406 N; VL = 1009N; BF = 258N; ST = 155N; MG = 157N; LG = 69N. The five loading conditions were (1) 50% of max force, (2) quadriceps weakness (75% of hamstrings and gastrocnemii forces along with 50% of maximum quadriceps force), (3) hamstrings weakness (75% quadriceps and gastrocnemii forces along with 50% of maximum hamstrings force), (4) 75% of max force, and (5) 100% of max force of all muscles. The muscle loading sequence was completely randomized inter-specimens but remained the same intra-specimens. These force profiles were applied to each specimen three times before and after ACL transection, cumulating to a total of 30 trials. Once the appropriate muscle load had been applied to all six muscle insertions, the axial load was increased at a rate of 60N/second up to 500 N, representing slightly more than half the applied body weight of the in vivo subject since 25% of gait occurs during double support.

Due to the very small changes in joint angle observed during pilot testing and high within specimen repeatability (ICC>0.92 trial to trial), the average joint angles were reported when the axial load achieved 500 N; to evaluate the effect of ACL transection on tibial translations, the average displacement during the loading sequence (mm) was reported. Since tibial plateau dimension differ between specimens, differences in contact area unrelated to the independent variable of load condition or ACL status would be expected, as such, the non-parametric Friedman test for paired samples was used to detect differences between the five muscle loading conditions ($p < 0.05$), with the independent variables being muscle forces and status of the ACL (SPSS V.16, IBM Corp.). The intra-articular dependent variables were mean contact area (medial: MCCA; lateral: LCCA; mm^2), mean contact pressure (medial: MCCP; lateral: LCCP; MPa), peak contact pressure (medial: MPCP; lateral: LPCP; MPa) exhibited on the medial and lateral condyles.

Results

The average joint angles (Table 3) and tibial translations (Table 4) displayed very repeatable results (within specimen ICC over 0.92 within loading condition) indicating that the application of muscle and axial loads causes a consistent interaction between the femur and tibia within loading condition. The relatively large between-specimen standard deviations in tables 3 and 4 can be attributed to a single specimen (specimen 2) whose flexion angle ranged from 2.36-3.47° during testing, which placed it as an outlier. We decided to keep it in the results so we conducted pairwise comparisons between ACL and no-ACL condition, rather than across specimen. The intra articular contact mechanics measured with the Tekscan pressure sensor for the ACL intact (ACL) and transected (NO ACL) are reported in Table 5.

Muscle loading: The Friedman test revealed that the amount of applied muscle force had a significant effect on tibiofemoral contact area and pressure when the ACL was intact: significant

differences were observed for MCCA, LCCA, MCCP, LCCP, MPCP and LPCP, with the interactions as determined using a Kruskal Wallis test reported in Table 7 (ACL). With the ACL removed, differences among muscle loads were only evident in MCCP and MPCP (Table 7, No ACL). The majority of these differences were in the 50% loading condition, which was significantly different from almost all other loading conditions for all dependent variables.

ACL status: The status of the ACL had a significant effect on tibiofemoral contact area (Table 5). Across all five loading conditions, MCCA significantly decreased ($P < 0.05$) from 436.7 mm^2 to 347.7 2 mm^2 after ACL transection while LCCA decreased from 521.8 mm^2 to 405.9 mm^2 after ACL transection. These differences were not seen in mean contact pressure as MCCP and LCCP (2.20 MPa and 2.18 MPa respectively) remained relatively unchanged after ACL removal (MCCP: 2.09 MPa; LCCP: 2.09 MPa). Differences were not seen in peak contact pressure as MPCP (ACL: 6.01 MPa; No ACL: 5.97 MPa) and LPCP (ACL: 7.78 MPa; No ACL: 8.04 MPa) remained stable after ACL transection.

Discussion

The aim of this study was to quantify the effect of altering simulated applied muscle load and ACL removal on the contact mechanics of the tibiofemoral joint using a simulator that allows these mechanics to be governed by the soft tissue constraints and applied loads. We applied five different muscle-loading profiles including simulated weakness on a lower limb to detect their effects on knee joint contact mechanics and kinematics. The simulator produced very repeatable joint angles and translations (ICCs > 0.92), while still being sensitive enough to detect increased contact areas and pressures when the applied muscle loads were increased. Furthermore, after ACL transection, we observed a decrease in tibiofemoral contact area with no corresponding change in contact pressure. The experimental protocol developed for this in-vitro study has been developed to allow the applied muscle forces acting on the knee joint to be the only contributors

to the production of measured contact mechanics. The UOKS has produced results demonstrating high reliability through very strong ICCs and provides results that concur with the current literature (Riegger-Krugh et al., 1998, Marzo & Gurske-DePerio, 2009) giving an indication that the experimental protocol used with the UOKS can potentially be recognized as a valid in-vitro knee simulation tool. Additionally, the combined muscle forces applied in the current study are greater than those of past studies, and it is through these large muscle loads that the tibiofemoral joint is most compressed. Even with the reduced axial load our combined internal and external forces results fall in the range of past studies for both contact area and pressure (Table 6) (Fukobayashi, 1980., Ahmed and Burke, 1983., Ihn, 1993., Riegger-Krugh, 1998., Portney and Watkins, 2000., Lee, 2006., Marzo and J. Gurske-DePerio, 2009, Morimoto, 2009., Poh, 2011). Changes were observed between muscle loading profiles for all contact variables in the ACL intact knee specimens; with the ACL removed, changes due to load were only observed for the MCCP and MPCP. However, Table 6 reveals that, in a majority of cases, the standard deviation, an indication of variability, increased with the ACL removal. We believe that this increase in variability indicates reduced joint stability, which is also supported by the values of Table 4, which, although not significant, showed increased tibial translations in all but two of the dependent variables. Both these explanations could have a similar interaction with the degenerative process since small changes in cartilage loading are associated with joint degeneration (Herzog and Longino, 2007). It may be that the relatively small (from a functional point of view) increases in translation and slightly altered rotation angles for the same applied loads, changes that would be undetectable using current gait analysis techniques (Benoit et al, 2007; Andersen et al 2010), are contributing to the degenerative process. Herzog and Federico (2006) state that "In vivo assessment of joint adaptive and degenerative responses to controlled in vivo loading produced through muscular stimulation is an essential and necessary stage in

gaining insight into the clinical problems of onset and progression of joint degeneration. Furthermore, we believe that the precise control of muscle forces (or the loss of muscle control through injury, muscle inhibition, reduced afferent feedback, or aging) is a factor contributing to joint degeneration leading to osteoarthritis." We are in agreement that increased knowledge on the impact of muscle strength alterations on the effects of knee joint contact mechanics is needed.

Comparing the ACL to non-ACL conditions, ACL removal resulted in a consistent decrease in medial and lateral contact area for all load conditions. Our results coincide with those of Hosseini et al (2012) who noted a reduced contact area after an ACL tear in vivo using a dual fluoroscopic and magnetic resonance imaging technique during weight-bearing. They reported the average tibial plateau contact area in the intact knee at low flexion angles was just over 500 mm^2 and was significantly reduced to slightly below 400 mm^2 in the ACL deficient state, which corroborate our in vitro results and lend validity to our protocol. Even with the observed decrease in contact area, contact pressures remained similar between ACL conditions. Stable pressure measurements following a decrease in contact area represents a decrease in net force measured by the sensor. Because the muscle loading profile and axial load applied to the specimen is unchanged across ACL condition, the applied external force to the knee joint remains the same. The observed decrease in net force between the femur and tibia might be explained by reviewing the complex role of the ACL (Cerulli et al, 2003), which not only restricts anterior tibial translation but applies a portion of its tension axially due to its insertion angle, effectively increasing joint compression, and could help explain the decreased contact areas following ACL removal.

While contact pressure (MCCP, LCCP, MPCP and LPCP) increased as expected with increasing muscle loads, the contact area did not consistently increase (Table 5). There are two plausible explanations: the first is that the small kinematic changes shift the centre of pressure on

the sensor, unweighting some cells and thus increasing the pressure on others; the second, and likely in conjunction with the first, is that pressure was distributed to contact areas that were not covered by the sensor. Should this have occurred, we acknowledge this as a study limitation. We limited this effect by ensuring the tekscan sensor is not repositioned after the sequence of loaded is initialized, and, through pilot tests, we determined that the sensor was in the optimal position where the femoral condyle contacts the tibial plateau. This is evidenced when reviewing the contact maps collected by the sesnors since it is clear that while loading occurred, the peak pressures areas were well circumscribed within the collectable data. Additionally, the tekscan sensor maps reveal that within every tested specimen, the shape of the contact area measured and the position of the peak pressures collected are consistently the same across the different muscles force profiles. Once a "map shape" change occurs, such as the transection of the ACL, it then remains the same throughout the different muscle force changes. We believe this is a good indication of repeatability demonstrated by the experimentation and, despite the limitations of the pressure sensing technology, evidence of the validity of our measures.

Another potential limitation with in vitro studies is the change in mechanical properties of the soft tissues within the joint, in particular due to dehydration. All efforts were made, including using wet compresses and continuous irrigation with a saline solution, to maintain fluids around the soft tissues. This was particularly applied between loading sequences as the joint decompressed. Given our similar contact areas when compared to Hosseini et al (2012) in vivo results, we are nevertheless confident that our in vitro simulation was capable of producing results which can be analogous to those expected in vivo with changes in muscle load and ACL status.

Conclusions:

We found that after removal of the ACL and despite very small (unmeasurable in the typical laboratory setting) changes in knee joint kinematics, alterations in soft tissue loading that could reasonably be associated with the degenerative process was recorded. Of particular note was the decrease in contact area after ACL transection, which warrants further investigation to determine if this reduced contact area is more susceptible to joint degradation and the onset of OA.

Acknowledgments

The authors would like to thank Hakim Louati of the Orthopedics Biomechanics Laboratory for all of his support throughout data collection and Brigitte Potvin with her assistance in data analysis. We would also like to thank the donors and their families for their generosity as without them, this and future studies could not happen. Financial support for this study was obtained from the Natural Sciences and Engineering Research Council (NSERC) of Canada and the Canadian Foundations for Innovation.

References

Lohmander, L. S. & Roos, H. 1994. Knee ligament injury, surgery and osteoarthrosis. Truth or consequences? Acta Orthopaedica Scandinavica 65: 605–609.

Hasler EM, Herzog W, Leonard TR, Stano A. & Nguyen H. 1998. In vivo knee joint loading and kinematics before and after ACL transection in an animal model. Journal of Biomechanics 31: 253-262.

Herzog W , Suter E,. 1997. Muscle Inhibition Following Knee Injury and Disease Sportverletzung-Sportschaden. 11, Issue 3, p 74-78

Herzog W, Longino D, Clark A, (2003) The role of muscles in joint adaptation and degeneration. Langenbeck's Archives of Surgery 338 (5) p. 305-315

Ageberg, E., Pettersson, A., Fridén, T. 2007. 15-Year follow-up of neuromuscular function in patients with unilateral nonreconstructed anterior cruciate ligament injury initially treated with rehabilitation and activity modification: A longitudinal prospective study. *American Journal of Sports Medicine*, 35 (12), pp. 2109-2117.

Lewis P.B., Parameswaran, A., Rue, J-P.H., Bach Jr., B.R. 2008. Systematic review of single-bundle anterior cruciate ligament reconstruction outcomes: A baseline assessmentfor consideratio n of double-bundle techniques. American Journal of Sports Medicine 36, (10), p. 2028-2036

Barenius, B., Nordlander, M., Ponzer, S., Tidermark, J., Eriksson, K. 2010. Quality of life and clinical outcome after anterior cruciate ligament reconstruction using patellar tendon graft or quadrupled semitendinosus graft: An 8-year follow-up of a randomized controlled trial. *American Journal of Sports Medicine*, 38 (8), pp. 1533-1541

Yoo J. D., Papannagari R., Park S. E., DeFrate L. E., Gill T. J. & Li G. 2005. The effect of anterior cruciate ligament reconstruction on knee joint kinematics under simulated muscle loads. American Journal of Sports Medicine 33 (2): 240–246.

Hsieh HH. & Walker PS. 1976. Stabilizing mechanisms of the loaded and unloaded knee joint. Journal of Bone and Joint Surgery 58: 93.

Markolf K. L., Mensch J. S. & Amstutz H. C. 1976. Stiffness and laxity of the knee–the contributions of the supporting structures. A quantitative in vitro study. Journal of Bone and Joint Surgery American 58 (5): 583–594.

Markolf K. L., Bargar W. L., Shoemaker S. C. & Amstutz H. C. 1981. The role of joint load in knee stability. Journal of Bone and Joint Surgery American 63 (4): 570–585.

Riegger-Krugh, C., Gerhart, T. N., Powers, W. R. & Hayes, W. C. 1998. Tibiofemoral contact pressures in degenerative joint disease. Clinical Orthopaedics and Related Research 348: 233–245.

Oh Y. K., Kreinbrink J. L., Ashton-Miller J. A. & Wojtys E. M. 2011. Effect of ACL transection on internal tibial rotation in an in vitro simulated pivot landing. Journal of Bone and Joint Surgery American 93 (4): 372–380.

Torzilli P. A. Deng X. & Warren R.F. 1994. The effect of joint-compressive load and quadriceps muscle force on knee motion in the intact and anterior cruciate ligament-sectioned knee. American Journal of Sports Medicine 22 (1): 105–112.

Withrow T. J., Huston L. J., Wojtys E. M. & Ashton-Miller J. A. 2006. The relationship between quadriceps muscle force, knee flexion, and anterior cruciate ligament strain in an in vitro simulated jump landing. American Journal of Sports Medicine 34 (2): 269–274.

Müller O., Lo J., Wünschel M., Obloh C. & Wülker N. 2009. Simulation of force loaded knee movement in a newly developed in vitro knee simulator Biomedizinische Technik 54 (3): 142–149.

Cassidy K, Hangalur G, Sabharwal P & Chandrashekar N. 2013. Combined in Vivo/in Vitro Method to Study Anteriomedial Bundle Strain in the Anterior Cruciate Ligament Using a Dynamic Knee Simulator. Journal of Biomechanical Engineering 135(3): 35001.

Brand R. A., Crowninshield R.D., Wittstock C. E., Pedersen D. R., Clark C. R. & van Krieken F. M. 1982. A model of lower extremity muscular anatomy. Journal of Biomechanical Engineering 104 (4): 304–310.

Benoit DL, Ramsey DK, Lamontagne M, et al. 2006. Effect of skin movement artifact on knee kinematics during gait and cutting motions measured in vivo. Gait and Posture 24: 152-164.

Buchanan, T. S., Lloyd, D. G., Manal, K. & Besier, T. F. 2005. Estimation of muscle forces and joint moments using a forward-inverse dynamics model. Medicine and Science in Sports and Exercise 37: 1911–1916.

Buchanan, T. S., Lloyd, D. G., Manal, K., & Besier, T. F. (2004). Neuromusculoskeletal modeling: Estimation of muscle forces and joint moments and movements from measurements of neural command. *Journal of Applied Biomechanics, 20*(4), 367-395.

Marzo, J. M., & Gurske-DePerio, J. (2009). Effects of medial meniscus posterior horn avulsion and repair on tibiofemoral contact area and peak contact pressure with clinical implications. *American Journal of Sports Medicine, 37*(1), 124-129.

Fukubayashi, T., & Kurosawa, H. (1980). The contact area and pressure distribution pattern of the knee. A study of normal and osteoarthrotic knee joints. *Acta Orthopaedica Scandinavica, 51*(6), 871-879.

Ahmed, A. M., & Burke, D. L. (1983). In-vitro measurement of static pressure distribution in synovial joints - part I: Tibial surface of the knee. *Journal of Biomechanical Engineering, 105*(3), 216-225.

Ihn, J. C., Kim, S. J., & Park, I. H. (1993). In vitro study of contact area and pressure distribution in the human knee after partial and total meniscectomy. *International Orthopaedics, 17*(4), 214-218.

Portney L.G, and Watkins M.P, *Foundations of Clinical Research: Applications to Practice*. Prentice Hall, 2000

Radin, E. L., Swann, D. A., Paul, I. L., & McGrath, P. J. (1982). Factors influencing articular cartilage wear in vitro. *Arthritis and Rheumatism, 25*(8), 974-980.

Lee, S. J., Aadalen, K. J., Malaviya, P., Lorenz, E. P., Hayden, J. K., Farr, J., .Cole, B. J. (2006). Tibiofemoral contact mechanics after serial medial meniscectomies in the human cadaveric knee. *American Journal of Sports Medicine, 34*(8), 1334-1344.

Morimoto, Y., Ferretti, M., Ekdahl, M., Smolinski, P., & Fu, F. H. (2009). Tibiofemoral joint contact area and pressure after single- and double-bundle anterior cruciate ligament reconstruction. *Arthroscopy - Journal of Arthroscopic and Related Surgery, 25*(1), 62-69.

Poh, S., Yew, K., A., Wong, P., K., Koh, S., J., Chia, S., Fook-Chong, S., & Howe, T. (2012). Role of the anterior intermeniscal ligament in tibiofemoral contact mechanics during axial joint loading. *Knee,* 19, (2), p 135-139.

Herzog, W. & Longino, D. 2007. The role of muscles in joint degeneration and osteoarthritis. Journal of Biomechanics 40 Suppl 1: S54–63.

Benoit, D.L., Ramsey D.K., Lamontagne, M, Xu, L., Wretenberg, P. & Renstrom, P. 2007. In vivo knee kinematics during gait reveals new rotation profiles and smaller translations. Clinical Orthopaedics and Related Research 454: 81-88.

Andersen MS, Benoit DL, Damsgaard M, Ramsey DK & Rasmussen J. 2010. Do kinematic models reduce the effects of soft tissue artefacts in skin marker-based motion analysis? An in vivo study of knee kinematics. Journal of Biomechanics 43 (2): 268-73.

Herzog, W., & Federico, S. (2006). Considerations on joint and articular cartilage mechanics. *Biomechanics and Modeling in Mechanobiology, 5*(2-3), 64-81.

Cerulli, G., Benoit, D. L., Lamontagne, M., Caraffa, A. & Liti, A. 2003. In vivo anterior cruciate ligament strain behaviour during a rapid deceleration movement: case report. Knee Surgery Sports Traumatology Arthroscopy 11: 307–311.

Hosseini, A., Van de Velde, S. K., Gill, T. J. & Li, G. 2012. Tibiofemoral cartilage contact biomechanics in patients after reconstruction of a ruptured anterior cruciate ligament. Journal of Orthopaedic Research 30: 1781–1788.

Table and Figure Captions

Table 1. Mean tibiofemoral angles for the five different muscle-loading profiles. Sagittal (Flex-Ext), Frontal (Abd-Add) and horizontal (Int-Ext rotation).

Table 2. Change in position of the tibial origin relative to the femoral origin (tibial translation) measured during the axial loading sequence from 200N up to 500N (loading rate approximately 60N/second) in all three planes of motion for the five different muscle-loading profiles.

Table 3. Average values for all six contact variables within each muscle loading condition. Medial and lateral compartment contact area (MCCA, LCCA), mean medial and lateral compartment contact pressures (MCCP, LCCP) and medial and lateral peak contact pressures (MPCP and LPCP). Asterisk indicates values significantly ($P < 0.05$) lower than the corresponding ACL intact condition.

Table 4. Standard deviations values for the 5 different loading conditions in each specimen and for all 6 measured contact variables. Bold cases indicate increased standard deviation once the ACL is removed. Medial and lateral compartment contact area (MCCA, LCCA), mean medial and lateral compartment contact pressures (MCCP, LCCP) and medial and lateral peak contact pressures (MPCP and LPCP).

Table 5. Variables identified as significantly different using the Friedman test were evaluated post-hoc analysis using a Kruskal Wallis test to identify interactions between loading conditions. Load condition 1-5 correspond to 50% all muscles; 75% all muscles + 50% quadriceps; 75% all muscles + 50% hamstrings; 75% all muscles; and 100% all muscles respectively.

Table 6. Collection of previous studies measuring contact mechanics at the tibiofemoral joint in comparison with the present study.

Figure 8: 1a) The femur is fixed with bismuth allow into the simulated hip joint. This joint is placed in a received attached to the axial loading device (BTS Model 858 Mini BionixEden Prairie, USA).

1b) The tibia and fibula are inserted into a simulated ankle joint and also secured with bismuth allow.

1c) Complete specimen along with marker triads; saline bathing clothes removed to clarity. Note that neither joint is held in place, nor are the surfaces of the joints fully covered, thus allowing biofidelic motion.

1d) University of Ottawa knee simulator from a posterior view. The pulley system allows to load the simulated muscles forces through the intended lines of action.

1e) Posterior-lateral view of the simulator. A better view of the guide pulley can be seen here.

1 Table 3

AVERAGE KNEE JOINT ANGLES (DEGREES)

LOADING CONDITIONS	Flex-Ext		Abd-Add		Int-Ext Rot.	
	ACL	NO-ACL	ACL	NO-ACL	ACL	NO-ACL
50% ALL	11.82±5.96	13.54±5.46	1.19±1.56	2.54±1.50	-6.78±4.14	-11.22±6.67
75% ALL + 50% QUAD	12.17±6.24	13.71±5.65	1.03±1.51	2.65±1.48	-6.97±4.15	-11.57±7.09
75% ALL + 50% HAMS	11.42±5.64	13.18±5.45	1.21±1.63	2.41±1.54	-6.84±4.25	-11.71±7.14
75% ALL	11.62±5.89	13.17±5.45	1.22±1.62	1.91±0.64	-6.83±4.26	-11.21±7.02
100% ALL	11.46±5.69	12.95±5.28	1.23±1.82	2.27±1.79	-6.87±4.60	-11.28±6.70

2
3
4 Table 4

TIBIAL TRANSLATIONS DURING AXIAL LOADING (MM)

LOADING CONDITIONS	Medial		Anterior		Distraction	
	ACL	NO-ACL	ACL	NO-ACL	ACL	NO-ACL
50% ALL	0.67±0.70	0.69±0.48	0.63±0.46	0.76±0.48	0.60±0.29	0.96±0.71
75% ALL + 50% QUAD	0.62±0.80	0.73±0.68	0.73±0.52	0.74±0.43	0.60±0.33	0.70±0.38
75% ALL + 50% HAMS	0.60±0.51	0.60±0.47	0.61±0.30	0.62±0.28	0.49±0.18	0.57±0.29
75% ALL	0.54±0.59	0.71±0.74	0.52±0.33	0.68±0.52	0.51±0.19	0.58±0.26
100% ALL	0.71±0.49	.090±1.15	0.71±0.36	0.78±0.74	0.56±0.35	0.46±0.12

5
6

1 Table 5

	ACL					
LOADING CONDITIONS	**MCCA (mm^2)**	**LCCA (mm^2)**	**MCCP (MPa)**	**LCCP (MPa)**	**MPCP (MPa)**	**LPCP (MPa)**
50% ALL	426.4	521.0	2.03	1.97	5.53	6.47
75% ALL + 50% QUAD	435.2	526.6	2.17	2.06	5.75	7.46
75% ALL + 50% HAMS	435.8	532.4	2.15	2.11	5.87	7.55
75% ALL	437.9	535.2	2.25	2.26	6.04	7.85
100% ALL	448.3	493.9	2.42	2.50	6.84	9.56
	NO ACL					
LOADING CONDITIONS	**MCCA (mm^2)**	**LCCA (mm^2)**	**MCCP (MPa)**	**LCCP (MPa)**	**MPCP (MPa)**	**LPCP (MPa)**
50% ALL	*354.3	*403.1	1.93	1.95	5.64	7.42
75% ALL + 50% QUAD	*356.1	*409.8	2.05	2.07	5.84	7.89
75% ALL + 50% HAMS	*344.0	*403.9	2.11	2.11	5.95	8.06
75% ALL	*345.3	*409.1	2.14	2.14	6.10	8.23
100% ALL	*338.9	*403.7	2.23	2.18	6.31	8.62

2
3

Table 6

		MCCA		LCCA		MCCP		LCCP		MCPCP		LCPCP	
		ACL	NO ACL	ACL	NO ACL	ACL	NO ACL	ACL	NO ACL	ACL	NO ACL	ACL	NO ACL
LOADING 1	spec1	**3,26**	**12,57**	6,19	4,39	**0,01**	**0,06**	**0,02**	**0,08**	**0,05**	**0,07**	**0,02**	**0,07**
	spec2	**14,32**	**44,00**	**17,65**	**41,83**	**0,10**	**0,25**	**0,11**	**0,33**	**0,46**	**0,74**	**0,55**	**2,61**
	spec3	5,31	4,76	7,96	4,43	0,02	0,02	**0,48**	**0,61**	0,08	0,04	**1,92**	**3,17**
	spec4	21,19	2,70	**5,07**	**27,42**	**0,06**	**0,16**	0,22	0,18	**0,04**	**1,07**	**0,16**	**0,57**
	spec5	9,07	2,78	**17,47**	**20,75**	0,41	0,03	0,18	0,10	0,91	0,28	4,78	0,25
	spec6	**5,30**	**9,14**	14,95	4,90	**0,22**	**0,48**	**0,11**	**0,62**	0,46	0,45	**0,40**	**1,01**
LOADING 2	spec1	**4,60**	**5,08**	**4,50**	**5,75**	**0,00**	**0,01**	0,04	0,02	**0,02**	**0,06**	**0,04**	**0,06**
	spec2	**1,70**	**48,49**	**2,07**	**36,12**	**0,06**	**0,25**	**0,12**	**0,35**	**0,45**	**0,70**	**0,43**	**2,48**
	spec3	**4,86**	**5,35**	**0,30**	**2,10**	0,01	0,00	**0,02**	**0,08**	**0,01**	**0,02**	**0,16**	**0,48**
	spec4	**4,84**	**6,80**	**1,10**	**3,38**	0,02	0,01	0,06	0,03	**0,09**	**0,12**	0,17	0,10
	spec5	**2,57**	**5,62**	**2,00**	**4,82**	**0,03**	**0,04**	**0,02**	**0,05**	0,12	0,09	0,28	0,00
	spec6	**7,56**	**9,53**	7,29	3,49	**0,12**	**0,13**	**0,05**	**0,15**	0,17	0,17	**0,08**	**0,35**
LOADING 3	spec1	**0,05**	**2,78**	**0,19**	**0,87**	**0,00**	**0,02**	0,01	0,01	**0,02**	**0,04**	**0,01**	**0,07**
	spec2	**12,33**	**37,12**	**4,17**	**24,58**	**0,04**	**0,22**	**0,04**	**0,54**	**0,23**	**0,48**	**0,23**	**4,41**
	spec3	**4,52**	**14,49**	**1,16**	**3,28**	**0,00**	**0,01**	**0,08**	**0,16**	0,01	0,01	**0,39**	**1,03**
	spec4	**6,39**	**16,90**	**3,49**	**4,08**	**0,04**	**0,05**	0,15	0,09	**0,04**	**0,47**	0,48	0,18
	spec5	4,54	2,57	**6,66**	**9,54**	0,13	0,06	0,06	0,03	**0,18**	**0,57**	1,04	0,08
	spec6	**1,63**	**12,58**	20,16	8,54	**0,09**	**0,23**	**0,08**	**0,09**	0,38	0,15	0,52	0,38
LOADING 4	spec1	**3,59**	**8,91**	**0,76**	**6,73**	**0,02**	**0,04**	0,04	0,03	**0,03**	**0,06**	**0,05**	**0,07**
	spec2	**6,60**	**34,35**	**4,06**	**29,94**	**0,02**	**0,22**	**0,03**	**0,53**	0,38	0,36	**0,90**	**4,66**
	spec3	15,17	12,49	**0,78**	**1,85**	0,01	0,00	0,11	0,09	0,05	0,02	**0,44**	**0,64**
	spec4	13,10	10,04	**4,32**	**4,52**	0,04	0,05	0,14	0,08	**0,02**	**0,35**	0,30	0,07
	spec5	4,33	3,04	**7,32**	**13,75**	0,22	0,07	**0,06**	**0,12**	**0,08**	**0,64**	1,29	0,49
	spec6	19,77	12,85	17,04	10,37	0,46	0,32	0,62	0,33	0,76	0,11	0,72	0,42
LOADING 5	spec1	2,91	2,90	1,99	1,89	0,02	0,00	0,02	0,00	0,03	0,03	0,04	0,01
	spec2	**1,62**	**2,62**	**3,11**	**4,10**	0,02	0,00	0,01	0,01	0,16	0,01	0,06	0,03
	spec3	**1,52**	**2,23**	**0,33**	**0,83**	0,00	0,00	0,06	0,05	0,01	0,00	0,33	0,06
	spec4	**0,33**	**3,68**	**0,05**	**0,68**	**0,01**	**0,02**	0,04	0,03	0,17	0,12	**0,18**	**0,22**
	spec5	**5,01**	**7,32**	**2,78**	**6,26**	**0,01**	**0,02**	**0,01**	**0,05**	0,13	0,12	0,01	0,00
	spec6	**0,28**	**3,09**	**1,50**	**2,84**	**0,04**	**0,06**	0,06	0,03	**0,09**	**0,13**	0,23	0,11

Table 7

ACL					NO ACL			
PAIRED LOADING	**MCCA**	**LCCA**	**MCCP**	**LCCP**	**MPCP**	**LPCP**	**MCCP**	**MPCP**
1_2	.014*	.020*	.001*	.016*	.039*	.016*	.020*	.306
1_3	.048*	.039*	.002*	.007*	.003*	.002*	.035*	.035*
1_4	.014*	.008*	.000*	.000*	.001*	.000*	.012*	.011*
1_5	.006*	.983	.000*	.000*	.000*	.001*	.028*	.011*
2_3	.811	.022*	.811	.184	.078	.711	.184	.983
2_4	.356	.003*	.010*	.002*	.010*	.078	.064	.085
2_5	.058	.845	.000*	.001*	.000*	.001*	.043*	.011*
3_4	.381	.199	.039*	.004*	.044*	.084*	.085	.005*
3_5	.133	.528	.000*	.001*	.000*	.001*	.010*	.053
4_5	.133	.316	.002*	.018*	.000*	.001*	.199	.085

Table 6

Studied variables	**Gauthier et al. (present study)**	**Kettlekamp (1972)**	**Fukubayashi Kurosawa (1980)**	**Ahmed and Burke (1983)**	**Ihn (1993)**	**Riegger-krugh (1998)**	**Lee (2006)**	**Marzo (2009)**	**Morimoto (2009)**	**Poh (2011)**
Applied Axial load	500N	1.4 to 5 Kg	1000 N	890 N	120 Kg	1960 N	1800 N	1800 N	1000 N	1800 N
Contact area (mm^2)										
Medial compartment	399.06	468	640	-	610	749	533	594	595.12	374
Lateral compartment	459.17	297	510	-	450	522	-	571	443.83	403
Medial & lateral compartments	858.23	765	1150	-	-	1371	-	1165	1038.95	777
Mean contact pressure (MPa)										
Medial compartment	1.67	-	-	1.38 - 2.07	-	2.52	1.77	-	3.49	3.61
Lateral compartment	2.82	-	-	1.38 - 2.07	-	3.86	-	-	3.66	1.93
Medial & lateral compartments	4.49	-	-	-	-	-	-	-	-	2.73

Figure 8

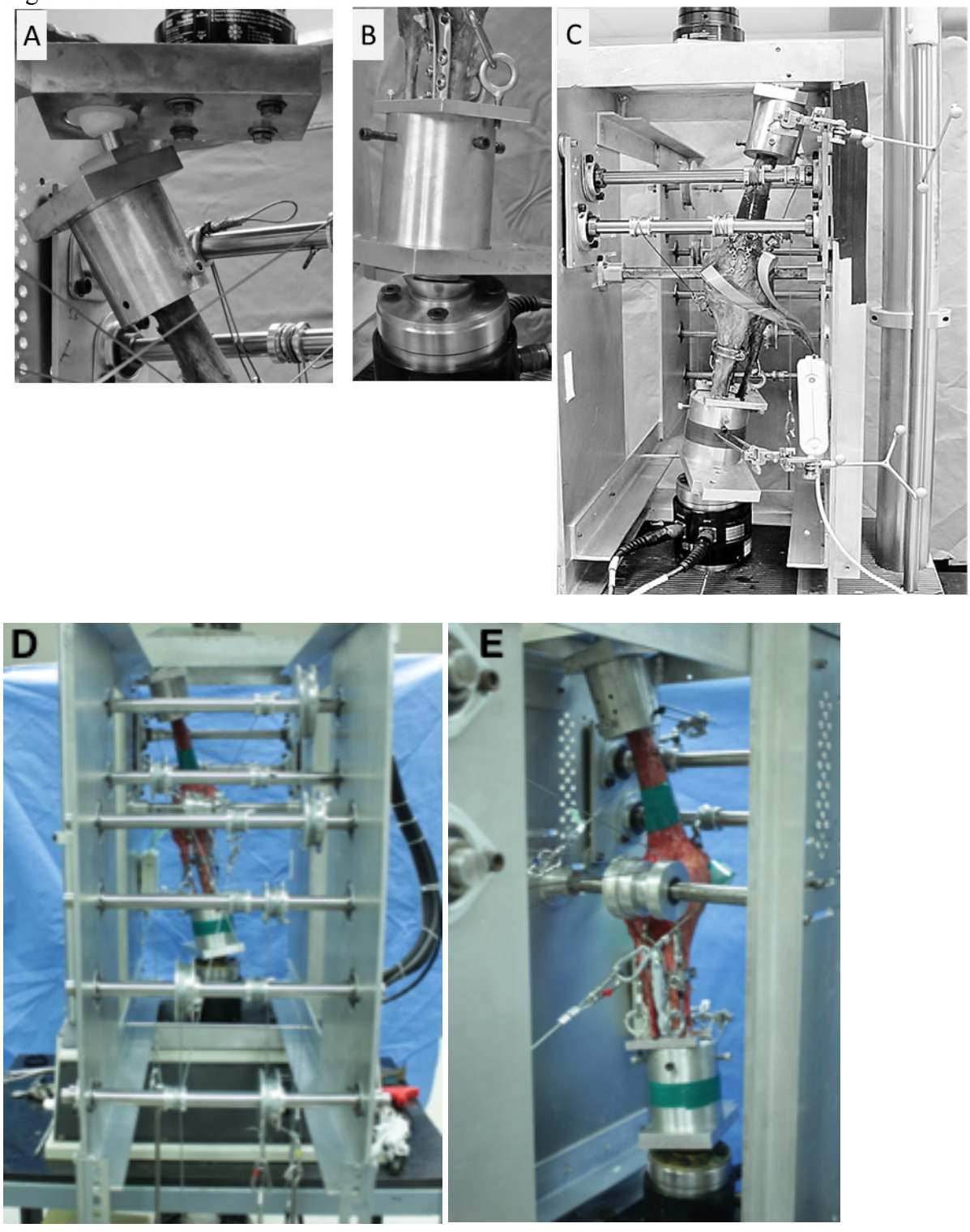

Appendix 1

Knee joint degeneration initiation and progression

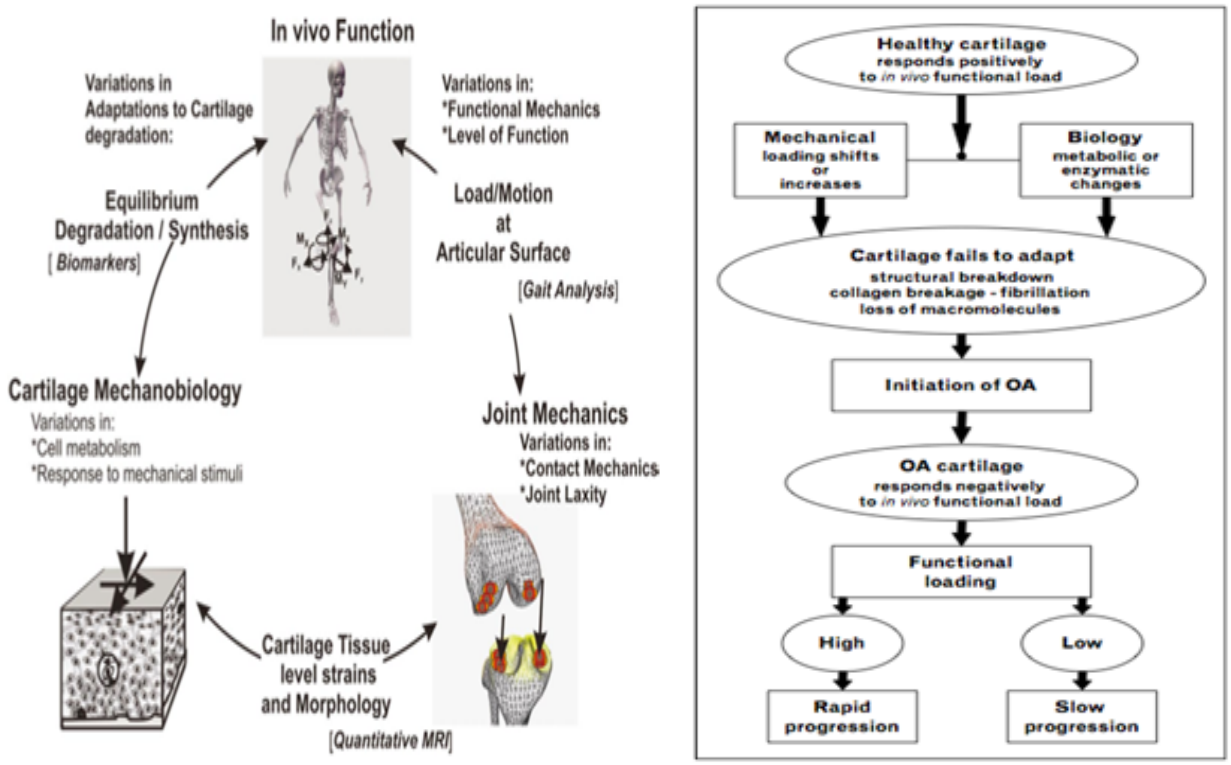

Figure 9. Framework representing the initiation and progression processes of OA developed by Andriacchi et al. (2004, 2006)

Appendix 2

Experimental protocol loading magnitudes, muscle tension profiles and examples of loading sequences

Table 8. Simulated muscle loads with pulley ratio and applied static loads to achieved desired muscle force simulation

Pulley ratios	Ratio	Weight (lbs)	Load pulley diameter	Static load (N)	Applied load (N)
Quadriceps					
Medial	2,03	45	48,72	200,17	406,30
Lateral	2,52	2x45	60,48	400,34	1008,90
Gastrocs					
Medial	3,54	10	84,96	44,48	157,46
Lateral	1,54	10	36,96	44,48	68,50
Hamstrings					
Medial	2,32	25	55,68	111,21	257,99
Lateral	1,39	25	33,36	111,21	154,57

Table 9. . Experimental protocol loading sequence with the UOKS.

Specimens # 1	50% of max. all muscles	75% all muscles + 50% of max. quads	75% all muscles + 50% of max. hams.	Max. muscle loading (100%)
Loading cycles				
1				
2				
3				
ACL resection				
4				
5				
6				

Table 10. Example of loading sequence with the UOKS.

	Muscle loading conditions														
ACL	**50% all muscles**			**75 % all & 50% quadriceps**			**75% all & 50% hamstrings**			**75% all muscles**			**100% all muscles**		
Intact	1	5	9	6	7	10	2	4	11	3	8	12	14	15	16
Removed	1	5	9	6	7	10	2	4	11	3	8	12	14	15	16

Appendix 3

Table 11. Comparison of in-vitro studies measuring tibiofemoral contact mechanics.

Studied variables	Gauthier et al. (present study)	Kettlekamp (1972)	Fukubayashi Kurosawa (1980)	Ahmed and Burke (1983)	Ihn (1993)	Riegger-krugh (1998)	Lee (2006)	Marzo (2009)	Morimoto (2009)	Poh (2011
Applied Axial load	500N	1.4 to 5 Kg	1000 N	890 N	120 Kg	1960 N	1800 N	1800 N	1000 N	1800 N
Contact area (mm^2)										
Medial compartment	399.06	468	640	-	610	749	533	594	595.12	374
Lateral compartment	459.17	297	510	-	450	522	-	571	443.83	403
Medial & lateral compartments	858.23	765	1150	-	-	1371	-	1165	1038.95	777
Mean contact pressure (MPa)										
Medial compartment	1.67	-	-	1.38 - 2.07	-	2.52	1.77	-	3.49	3.61
Lateral compartment	2.82	-	-	1.38 - 2.07	-	3.86	-	-	3.66	1.93
Medial & lateral compartments	4.49	-	-	-	-	-	-	-	-	2.73

Appendix 4

Virtual landmark digitization and segments creation

1-2. Lateral aspects of femoral shaft measured by largest diameter of the femur observable between the two horizontal loading shafts.
3-4. Most distal aspects of the medial and lateral femoral condyles;
5-6. Medial and lateral edges of proximal tibia;
7-8. Lateral aspects of tibia measured by largest diameter of the tibia.
9. Femoral inter-condylar notch
10. Tibial eminence
These anatomical landmarks are identified using a probing instrument recognized by the motion tracking system. Local coordinate systems of the femur and tibia were defined as follows:

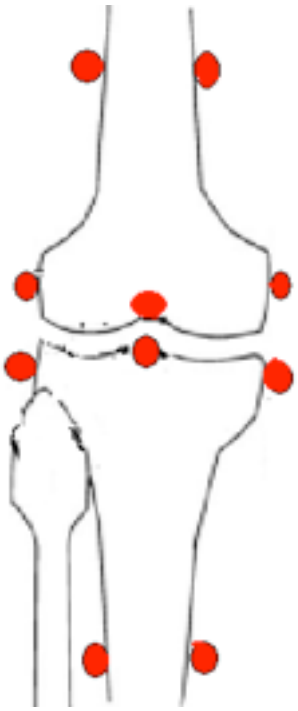

Xf: cross product of vectors Zf and Yf; from the femoral origin, directed laterally.
Yf: cross product of Zf and vector joining points 1 and 2; from the femoral origin, directed anteriorly.
Zf: vector joining points 3 and 4; from the femoral origin directed longitudinally along the femoral axis in the frontal plane.
Xt: cross product of vectors Zt and Yt; from the tibial origin, directed laterally.
Yt: cross product of Zt and vector joining points 5 and 6; from the tibial origin, directed anteriorly.
Zt: vector joining points 7 and 8; from the tibial origin directed longitudinally along the tibial axis in the frontal plane

Figure 10. Virtual landmarks to be digitized (red, above) and segment reference system and tracking technique based on Benoit et al. 2006.

Appendix 5

Visual 3D: create segments from manual digitisation's

1. Open V3D.

2. Open pipeline and select "01_Load_landmarks.v3s".

3. Execute pipeline. There are two prompts:
4. Select static trial,
5. Select Potted and Full leg trials.

6. In Model tab, click the "Model Builder Post Process" on the tool bar.

7. Click the "Add a Motion File from the Workspace" and select the potted trial.

8. Create events (virtual landmarks). Advance motion file to the first pointed landmark and click "add event at current frame". The secondary window that pops up - move it to a corner of the screen so you can still see the 3D viewer window.

9. Define events for each landmark.

10. Click "Compute ALL Landmarks".

11. Close Events window and Model Builder Post Processing window

12. Select the Signal and Event processing tab, and select the Full_leg trial, graph the Tip data.

13. Add the remaining events - FEM_HEAD, G_TROCH, INTER_COND, TIB_EMI, LAT_ankle, MED_ankle

14. Open pipeline window. Clear pipeline and open the second pipeline named: 02_Determine_pos_from_Full_leg_trial.v3s

15. Execute. This creates metric data for the model using the events defined in 11.
16. Clear pipeline and open "03_Add_landmarks_and creates segments". Execute pipeline. This adds the new landmarks and creates the segments.

17. Add all specimen motion files to V3D workspace. Click open new file. Insert new files into currently open workspace. Select all motion files. Assign model template to all specimen motion files.

18. Chose motion file in drop-down folder at top right hand on V3D interface.

19. Load “compute tibia translations” pipeline. Execute.

20. Load “data processing” pipeline. Execute.

21. Export data to ASCII file.

Appendix 6

Tekscan calibration and analysis manual

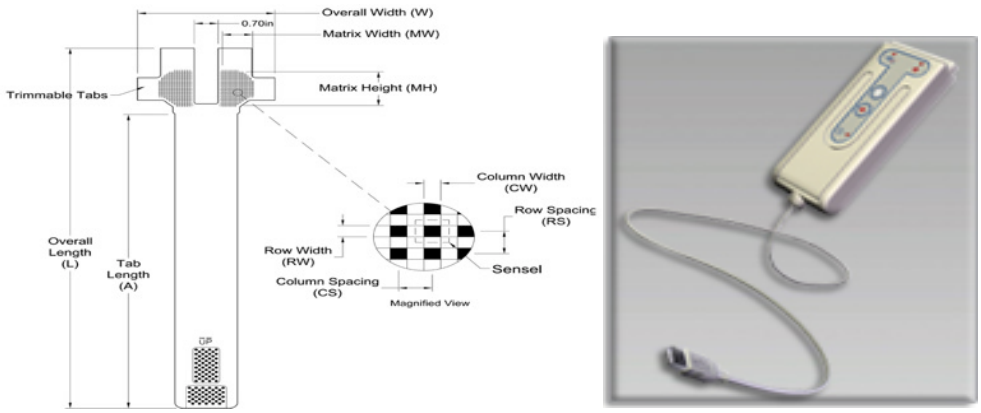

Figure 11 Tekscan 4011 sensor and USB evolution handle (Tekscan inc. South Boston, MA)

1. Open Tekscan software, I-scan 5.83 version
2. Chose movie file
3. Apply equilibration file first then apply appropriate calibration file. The appropriate calibration file corresponds to the sensor sensitivity used during data collection. (This is a critical aspect of data collection because it is not possible to calibrate the sensor in its testing environment as recommended by Tekscan Inc. The solution to this is to use actual loading sequences to observe if the sensor sensels will saturate. Then the appropriate sensitivity is used for the official data collection)
4. Confirm that the appropriate measuring units are selected by clicking this icon  in the toolbar. Select Newtons and MPas.
5. Add first "data box" by selecting  in the toolbar
6. This first data box is green and will remain on the left sensor of the movie. It will correspond to the medial or lateral condyle depending if a right or a left knee specimen is used. This must be noted.
7. Add a second data box by selecting the same icon.
8. Expand both data boxes to cover their respective sensor.
9. Select both boxes and click export to ASCII.
10. You will be prompted to select the appropriate data to export.
11. When exporting center of force (COF) data. Verify that the boxes option is selected in the properties option  . 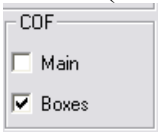

Appendix 7

Table 12. Specimen anthropometric data

	Specimen 2241		*Specimen 2250*		*Specimen 2359*	
Gender	***Male***		***Male***		***Female***	
Age	***66***		***65***		***67***	
	left knee	***right knee***	***left knee***	***right knee***	***Left knee***	***Right knee***
full leg length	*88.8*	*90*	*82*	*83*	*79*	*78.8*
femur length	*48.7*	*49.5*	*44.5*	*44.5*	*43.2*	*43*
tibia length	*40.8*	*40*	*38*	*38*	*36.5*	*35.9*
femoral condyle width	*9.1*	*9.3*	*9.2*	*9.4*	*7.5*	*7.9*
tibial plateau width	*8*	*8.2*	*8.9*	*8.2*	*6.5*	*6.7*
malleoli width	*7*	*6.2*	*7.1*	*7.1*	*5.5*	*5.6*

Appendix 8

Detailed experimental protocol

Knee Dissection

- Reach hip joint and separate form cadaver
- Remove foot
- Remove all skin, adipose tissue and musculature
- Dissect around the patella to reach the patellar tendon, remove all excess soft tissue and adipose tissue that could hinder access to tibio-femoral joint
- Keep collateral ligaments intact
- Open posterior capsule (access to joint line)
- Remove excess soft tissue lining that covers the patellar bone (facilitates muscle insertion placement)
- Transport lower limb to Biomechanics lab
- Measure full lower limb dimensions
    - Femur length (femoral head to tib-fem joint line)
    - Femur width at condyles and mid-shaft
    - Tibia Length (tib-fem joint line to distal malleoli)
    - Tibia width at plateau and mid-shaft
    - Photos

Pressure sensor Equilibration and Calibration

- Open I-scan 5.83
- Cut Tekscan 4011 sensor tab down the middle in the non-sensing area
- Also cut the lateral non-sensing tabs around the sensing area
- Install Tekscan sensor into USB handle
- Install calibration setup with steel sphere, metal plates and cork lining
- Load Sensor with 500N and wait 5 minutes, repeat twice for 15 minutes of total condition time
- Calibration must be performed at different sensitivity settings, e.g., mid-1, mid-2 and default sensitivities
- Select sensitivity
- Equilibrate sensor, (save equilibration)
- Select calibration and apply 2-point power law calibration at 200N and 800N
- Save calibration file to specimen identification and sensor identification
- Repeat with different sensitivities (New equilibration is needed)

Vicon Motion Capture calibration

- Install 5 Vicon cameras and Power On Vicon system
- Check for ghost markers and create mask
- Calibrate Vicon system without the Knee simulator in place
- Set volume origin

Full limb virtual landmark digitization

- Use a permanent marker on bone segments to identify the virtual landmarks as well as the following 4 landmarks that apply to the full lower limb: femoral head (superior border of the ligamentum teres), greater trochanter, medial malleolus and lateral malleolus.
- Place the specimen on a supporting tray in the camera field of view at approximately 30 degrees of flexion.
- Collect a "Static trial" while holding the digitizing pointer in the field of view.
- Record a single motion file identifying all the landmarks in the following order
    1. Femoral head
    2. Medial Femur
    3. Medial Condyle
    4. Medial Plateau
    5. Medial Tibia
    6. Medial malleolus
    7. Greater trochanter
    8. Lateral Femur
    9. Lateral Condyle
    10. Lateral Plateau
    11. Lateral Tibia
    12. Lateral malleolus
    13. ACL femur insertion
    14. ACL tibia insertion

Knee Potting

- Section femur and tibia 26 cm above and below joint line
- Place bismuth in water tub, on heating plate, for melting
- Screw bone plates in position (see annexe 4 for further details)
    - Patella
    - Bilateral Hamstrings
    - Add plumber's clamp
- Install Kinematic bone pins into tibia and femur metal fixtures
- Once bismuth is liquid, align the femur in its corresponding metal pot and carefully pour in bismuth
- Repeat with the tibia (the fibula will be lying against the inner wall of the pot)
- Wait until bismuth is solidified
- Add remaining potting plates and rings accordingly to accommodate for left or right specimen

Hydraulic Load-frame

- Turn on MTS hydraulic load cell and load warm procedure (300 cycles)
- Power On refrigerated re-circulator (see order below)

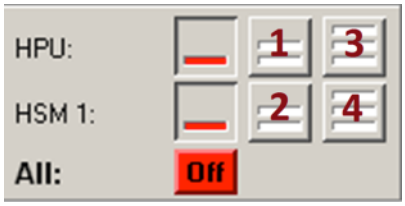

Figure 12. Power on refrigerated circulator order

- Lower the horizontal crosshead manually to desired height for sensor calibration
- Manually adjust the loading shaft to desired height
- Calibrate the Tekscan 4011 pressure sensor (see following section)

Serrated wire insertion

- Once the knee is potted and the bismuth is cooled. Use curved Kelly forceps to pass the wire behind the ACL.
- Place both ends of the wire along the femur shaft and use adhesive tape to keep the wire in place for the ACL retaining loading sequence.

Tekscan sensor placement in specimen

- It is safer to install the pressure sensor once the serrated wire is in place. Reversing these steps increases the risk of damaging the sensor.
- Place the potted knee on a steady surface.
- With a thin pair of forceps, reach through the knee joint posterior to anterior.
- Grab the non-sensing tab component of the sensor and pulled the sensor onto the tibial plateau.
- Once the desired position is achieved, apply super-glue on the underside of the non-sensing tab.
- Glue the tab downwards onto the posterior aspect of the tibial plateau.
- Repeat for the second compartment.

Knee simulator

- Adjust the knee simulator to accommodate for left or right knee
  - Add concave foot insert onto the MTS load cell
  - Add acetabulum simulation piece MTS to load cell
- Install the U of O knee simulator onto the MTS load-frame
- Install Knee inside the knee simulator
- Add 2,5 kg weights to suspend knee
- Add the *Brainlab (BrainlabAG, Feldkirchen, Germany)* bone pin guiding tools and adjust for distance

- Add the marker tracking tools and lock into place
- Insert sensor into USB handle, attach handle to simulator
- Adjust knee position and acetabular placement to 10-15 degrees of sagittal knee flexion using the manual command for the hydraulic loading system

Potted virtual landmark digitization in the UOKS

- Once the knee is installed in the UOKS, collect a "Static trial" while holding the digitizing pointer in the field of view.
- Record a single motion file identifying all the "potted" landmarks in the following order
    1. Medial Femur
    2. Medial Condyle
    3. Medial Plateau
    4. Medial Tibia
    5. Lateral Femur
    6. Lateral Condyle
    7. Lateral Plateau
    8. Lateral Tibia
    9. ACL femur insertion
    10. ACL tibia insertion

Data collection

- Load Tekscan I-scan 5.83 software
- Select New recording
- In MTS Station Manager, open .UOKneeSim MTS Procedure
- In Nexus software, create a new trial in data management
- Add weights to muscles for desired loading conditions (see Appendix 2, Table 9 and Table 10 for a loading sequence example)
- Start Tekscan recording (150 frames = 30 seconds) 5 HZ
- Start collecting kinematic data in Nexus 100HZ
- Start .UOKneeSim procedure
    - 5 second ramp up to 500N
    - 10 second hold at 500N
    - 5 second ramp down to 200 N
- Save Trial in Nexus
- Save Movie in I-Scan
- Repeat for all conditions three times

Following intact ACL knee loading

- Unload the knee to 2,5 kg weights
- Inspect muscle attachments
- Detach patella from medial and lateral quadriceps loading cables
- Use previously installed serrated wire to cut through the ACL
- Reposition knee
- Repeat the data collection steps

Appendix 9

Intraclass correlation coefficient analyses tables

Table 13. ICC values for contact variables with ACL intact

LOADING	MCCA	LCCA	MCCP	LCCP	MPCP	LPCP
1	.997	.991	.998	.994	.997	.932
2	.999	.999	.999	.999	.999	.999
3	.999	996	.999	.999	.999	.993
4	.996	.995	.998	.991	.998	.99
5	.999	.999	.999	.999	.999	.999

Table 14. ICC values for contact variables with ACL removed

LOADING	MCCA	LCCA	MCCP	LCCP	MPCP	LPCP
1	.992	.995	.996	.972	.995	.933
2	.991	.998	.999	.995	.999	.977
3	.993	.999	.999	.991	.998	.928
4	.994	.998	.998	.987	.999	.926
5	.999	.999	.999	.999	.999	.999

Table 15. ICC values for kinematic data with ACL intact

	KNEE ANGLES			KNEE TRANSLATIONS		
LOADING	FLEX-EXT	ABD-ADD	MED-LAT ROT	MEDIO-LAT	A-P	DIST-COMP
1	.999	.990	.999	.973	.999	.999
2	.999	.999	.998	.992	.999	.999
3	.999	.997	.999	.987	.999	.999
4	.999	.998	.999	.995	.999	.999
5	.999	.999	.999	.95	.999	.998

Table 16. ICC values for kinematic data with ACL removed

	KNEE ANGLES			KNEE TRANSLATIONS		
LOADING	FLEX-EXT	ABD-ADD	MED-LAT ROT	MEDIO-LAT	A-P	DIST-COMP
1	.999	.995	.999	.950	.986	.999
2	.999	.999	.999	.967	.997	.999
3	.999	.999	.999	.975	.998	.999
4	.999	.999	.999	.994	.999	.999
5	.999	.997	.999	.972	.988	.999

Appendix 10

Muscle insertion placement

Materials needed

- 1 “T” shaped bone plate
- 4, ¼ inch length, bone screws
- 2 “U” shaped bolt
- 2 curved bone plates

Procedure

1. Place the “T” shaped bone plate centrally on the patella to attach the simulated quadriceps.

2. 4 bone screws are used to secure the quadriceps “T” shaped bone plate.

3. “U” shaped bolts secured to the patella “T” shaped bone plate for the medial and lateral quadriceps attachments.

4. 2 curved bone plates are placed posteriorly on the tibia. The lateral plate will be positioned with the proximal hole aligned with the head of the fibula to reproduce the lateral hamstring insertion site.

5. The medial bone plate is positioned on the medial limit of the posterior wall of the tibia. It is aligned 2 cm distal to the tibial plateau simulating the medial hamstring muscle group.

6. Both gastrocnemius muscle insertions are determined from the design of the computer assisted design (CAD) software and are found on the foot and ankle fixation cup.

Appendix 11

Specimen potting to fixtures

Femur components

- 70 mm fixture cup with 5 alignment screws
- Femoral head and neck plate with 3 screws to fixture cup

Tibial and fibular components

- 90 mm fixture cup with 4 alignment screws
- Foot and ankle plate with 4 screws to fixture cup
- Partial-sphere foot component

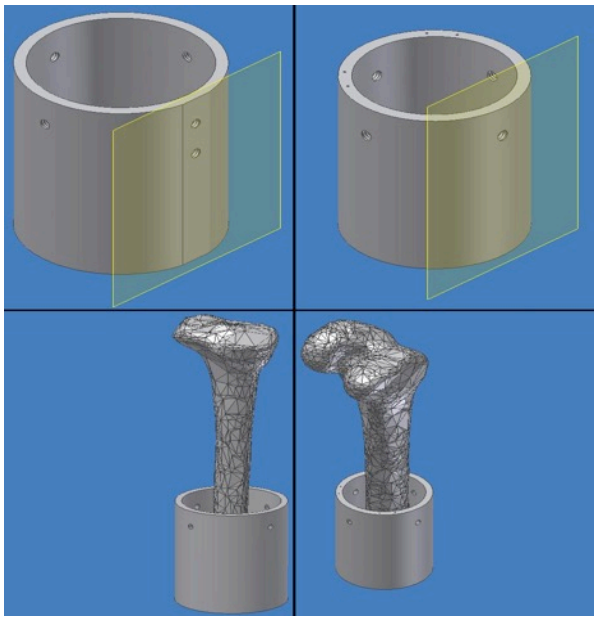

Figure 13. Fixation cups for the tibia (left) and the femur (right). Planes shown in top two figures are the frontal planes placed at the front of the cup for each cup. The bottom two figures demonstrate the limb alignment in the cup for each limb. Note that fixation cups are rotated 90 deg. from the top to bottom figures.

References

Ahmed, A. M., & Burke, D. L. (1983). In-vitro measurement of static pressure distribution in synovial joints - part I: Tibial surface of the knee. *Journal of Biomechanical Engineering, 105*(3), 216-225.

Alhalki, M. M., Hull, M. L., & Howell, S. M. (2000). Contact mechanics of the medial tibial plateau after implantation of a medial meniscal allograft: A human cadaveric study. *American Journal of Sports Medicine, 28*(3), 370-376.

Anderson, F. C., & Pandy, M. G. (2003). Individual muscle contributions to support in normal walking. *Gait and Posture, 17*(2), 159-169.

Andriacchi, T. P., Briant, P. L., Bevill, S. L., & Koo, S. (2006). Rotational changes at the knee after ACL injury cause cartilage thinning. *Clinical Orthopaedics and Related Research,* (442), 39-44.

Andriacchi, T. P., Mündermann, A., Smith, R. L., Alexander, E. J., Dyrby, C. O., & Koo, S. (2004). A framework for the in vivo pathomechanics of osteoarthritis at the knee. *Annals of Biomedical Engineering, 32*(3), 447-457.

Asano, T., Akagi, M., Tanaka, K., Tamura, J., & Nakamura, T. (2001). In vivo three-dimensional knee kinematics using a biplanar image-matching technique. *Clinical Orthopaedics and Related Research,* (388), 157-166.

Ateshian, G. A. (1994). A stereophotogrammetric method for determining in situ contact areas in diarthrodial joints, and a comparison with other methods. *Journal of Biomechanics, 27*(1), 111-124.

Bach, J. M., & Hull, M. L. (1994). Description and evaluation of a new load application system for in vitro study of ligamentous injuries to the human knee joint. *American Society of Mechanical Engineers, Bioengineering Division (Publication) BED, 28* 283-284.

Bachus, K. N., DeMarco, A. L., Judd, K. T., Horwitz, D. S., & Brodke, D. S. (2006). Measuring contact area, force, and pressure for bioengineering applications: Using Fuji film and TekScan systems. *Medical Engineering and Physics, 28*(5), 483-488.

Baratta, R., Solomonow, M., Zhou, B. H., Letson, D., Chuinard, R., & D'Ambrosia, R. (1988). Muscular coactivation. The role of the antagonist musculature in maintaining knee stability. *Am J Sports Med, 16*(2), 113-22.

Bartel, D. L., Bicknell, V. L., & Wright, T. M. (1986). The effect of conformity, thickness, and material on stresses in ultra-high molecular weight components for total joint replacement. *Journal of Bone and Joint Surgery - Series A, 68*(7), 1041-1051.

Bei, Y., & Fregly, B. J. (2004). Multibody dynamic simulation of knee contact mechanics. *Medical Engineering and Physics, 26*(9 SPEC.ISS.), 777-789.

Benoit DL, Ramsey DK, Lamontagne M, Xu L, Wretenberg P, Renström P. (2006). Effect of skin movement artifact on knee kinematics during gait and cutting motions measured in vivo. (2006). *Gait and Posture, 24*(2), 152-164.

Benoit, D. L., Ramsey, D. K., Lamontagne, M., Xu, L., Wretenberg, P., & Renström, P. (2007). In vivo knee kinematics during gait reveals new rotation profiles and smaller translations. *Clinical Orthopaedics and Related Research,* (454), 81-88.

Bergmann G, Bender A, Graichen F, Dymke J, Rohlmann A, Trepczynski A, Heller M.O, Kutzner, I. (2014). Standardized loads acting in knee implants. PLoS One. 9, (1)

Biau, D. J., Tournoux, C., Katsahian, S., Schranz, P., & Nizard, R. (2007). ACL reconstruction: A meta-analysis of functional scores. *Clinical Orthopaedics and Related Research,* (458), 180-187.

Brady, M. F., Bradley, M. P., Fleming, B. C., Fadale, P. D., Hulstyn, M. J., & Banerjee, R. (2007). Effects of initial graft tension on the tibiofemoral compressive forces and joint position after anterior cruciate ligament reconstruction. *American Journal of Sports Medicine, 35*(3), 395-403.

Brand, R. A., Crowninshield, R. D., Wittstock, C. E., Pedersen, D. R., Clark, C. R., & Van Krieken, F. M. (1982). Model of lower extremity muscular anatomy. *J BIOMECH ENG TRANS ASME, V 104*(N 4), 304-310.

Briem, K., Ramsey, D. K., Newcomb, W., Rudolph, K. S., & Snyder-Mackler, L. (2007). Effects of the amount of valgus correction for medial compartment knee osteoarthritis on clinical outcome, knee kinetics and muscle co-contraction after opening wedge high tibial osteotomy. *Journal of Orthopaedic Research, 25*(3), 311-318.

Brimacombe, J. M., Wilson, D. R., Hodgson, A. J., Ho, K. C. T., & Anglin, C. (2009). Effect of calibration method on tekscan sensor accuracy. *Journal of Biomechanical Engineering, 131*(3)

Buchanan, T. S., Lloyd, D. G., Manal, K., & Besier, T. F. (2004). Neuromusculoskeletal modeling: Estimation of muscle forces and joint moments and movements from measurements of neural command. *Journal of Applied Biomechanics, 20*(4), 367-395.

Burgess, I. C., Kolar, M., Cunningham, J. L., & Unsworth, A. (1997). Development of a six station knee wear simulator and preliminary wear results. *Proceedings of the Institution of Mechanical Engineers, Part H: Journal of Engineering in Medicine, 211*(1), 37-47.

Cerulli, G., Caraffa, A., Cerulli, G., Liti, A., Benoit, D. L., & Lamontagne, M. (2003). In vivo anterior cruciate ligament strain behaviour during a rapid deceleration movement: Case report. *Knee Surgery, Sports Traumatology, Arthroscopy, 11*(5), 307-311.

Clark, A. L., Herzog, W., & Leonard, T. R. (2002). Contact area and pressure distribution in the feline patellofemoral joint under physiologically meaningful loading conditions. *Journal of Biomechanics, 35*(1), 53-60.

Clark, A. L., Leonard, T. R., Barclay, L. D., Matyas, J. R., & Herzog, W. (2005). Opposing cartilages in the patellofemoral joint adapt differently to long-term cruciate deficiency: Chondrocyte deformation and reorientation with compression. *Osteoarthritis and Cartilage, 13*(12), 1100-1114.

Clark, A. L., Leonard, T. R., Barclay, L. D., Matyas, J. R., & Herzog, W. (2006). Heterogeneity in patellofemoral cartilage adaptation to anterior cruciate ligament transection; chondrocyte shape and deformation with compression. *Osteoarthritis and Cartilage, 14*(2), 120-130.

Clayton, R. A. E., & Court-Brown, C. M. (2008). The epidemiology of musculoskeletal tendinous and ligamentous injuries. *Injury, 39*(12), 1338-1344.

Collins, J. E., Katz, J. N., Donnell-Fink, L. A., Martin, S. D., & Losina, E. (2013). Cumulative incidence of ACL reconstruction after ACL injury in adults: Role of age, sex, and race. *American Journal of Sports Medicine, 41*(3), 544-549.

DiAngelo, D. J., & Harrington, I. A. (1992). Design of a dynamic multi-purpose joint simulator. *American Society of Mechanical Engineers, Bioengineering Division (Publication) BED, , 22* 107-110.

D'Lima, D. D., Steklov, N., Fregly, B. J., Banks, S. A., & Colwell Jr., C. W. (2008). In vivo contact stresses during activities of daily living after knee arthroplasty. *Journal of Orthopaedic Research, 26*(12), 1549-1555.

Donahue, T. L. H., Hull, M. L., Rashid, M. M., & Jacobs, C. R. (2002). A finite element model of the human knee joint for the study of tibio-femoral contact. *Journal of Biomechanical Engineering, 124*(3), 273-280.

Dressler, J.L., Ng, R.T, Amirfazli, A., & Carey, J.P., (2010). Development and evaluation of a multi-axis biomechanical testing apparatus for knee. Int.J. Experimental and computational biomechanics, Vol, 1, No. 3, 271-295

Fithian, D. C., Paxton, E. W., Stone, M. L., Luetzow, W. F., Csintalan, R. P., Phelan, D., & Daniel, D. M. (2005). Prospective trial of a treatment algorithm for the management of the anterior cruciate ligament-injured knee. *American Journal of Sports Medicine, 33*(3), 335-346.

Fitzgerald, G. K., Piva, S. R., & Irrgang, J. J. (2004). Reports of joint instability in knee osteoarthritis: Its prevalence and relationship to physical function. *Arthritis Care and Research, 51*(6), 941-946.

Freeman, M. A. R., & Pinskerova, V. (2005). The movement of the normal tibio-femoral joint. *Journal of Biomechanics, 38*(2), 197-208.

Frobell, R. B., Roos, E. M., Roos, H. P., Ranstam, J., & Lohmander, L. S. (2010). A randomized trial of treatment for acute anterior cruciate ligament tears. *New England Journal of Medicine, 363*(4), 331-342.

Frobell, R. B., Roos, H. P., Roos, E. M., Roemer, F. W., Ranstam, J., & Lohmander, L. S. (2013). Treatment for acute anterior cruciate ligament tear: Five year outcome of randomised trial. *BMJ (Online), 346*(7895)

Fukubayashi, T., & Kurosawa, H. (1980). The contact area and pressure distribution pattern of the knee. A study of normal and osteoarthrotic knee joints. *Acta Orthopaedica Scandinavica, 51*(6), 871-879.

Glitsch, U., & Baumann, W. (1997). The three-dimensional determination of internal loads in the lower extremity. *Journal of Biomechanics, 30*(11-12), 1123-1131.

Griffin, L. Y., Agel, J., Albohm, M. J., Arendt, E. A., Dick, R. W., Garrett, W. E., . . . Wojtys, E. M. (2000). Noncontact anterior cruciate ligament injuries: Risk factors and prevention strategies. *The Journal of the American Academy of Orthopaedic Surgeons, 8*(3), 141-150.

Griffin, T. M., & Guilak, F. (2005). The role of mechanical loading in the onset and progression of osteoarthritis. *Exercise and Sport Sciences Reviews, 33*(4), 195-200.

Guess, T. M., & Maletsky, L. P. (2005). Computational modelling of a total knee prosthetic loaded in a dynamic knee simulator. *Medical Engineering and Physics, 27*(5), 357-367.

Hamill, J. and Knutzen, KM., (2009) Biomechanical Basis of human movement, Third edition. Baltimore, USA. Lippincott Williams and Wilkins.

Harris, M. L., Morberg, P., Bruce, W. J. M., & Walsh, W. R. (1999). An improved method for measuring tibiofemoral contact areas in total knee arthroplasty: A comparison of K-scan sensor and fuji film. *Journal of Biomechanics, 32*(9), 951-958.

Hashemi, J., Chandrashekar, N., Jang, T., Karpat, F., Oseto, M., & Ekwaro-Osire, S. (2007). An alternative mechanism of non-contact anterior cruciate ligament injury during jump-landing: In-vitro simulation. *Experimental Mechanics, 47*(3), 347-354.

Hasler, E. M., & Herzog, W. (1998). Quantification of in vivo patellofemoral contact forces before and after ACE transection. *Journal of Biomechanics, 31*(1), 37-44.

Hasler, E. M., Herzog, W., Leonard, T. R., Stano, A., & Nguyen, H. (1998). In vivo knee joint loading and kinematics before and after ACL transection in an animal model. *Journal of Biomechanics, 31*(3), 253-262.

Heinlein, B., Graichen, F., Bender, A., Rohlmann, A., & Bergmann, G. (2007). Design, calibration and pre-clinical testing of an instrumented tibial tray. *Journal of Biomechanics, 40*(SUPPL. 1), S4-S10.

Herzog, W., Adams, M. E., Matyas, J. R., & Brooks, J. G. (1993). Hindlimb loading, morphology and biochemistry of articular cartilage in the ACL-deficient cat knee. *Osteoarthritis Cartilage, 1*(4), 243-51.

Herzog, W., Diet, S., Suter, E., Mayzus, P., Leonard, T. R., Muller, C., . . . Epstein, M. (1998). Material and functional properties of articular cartilage and patellofemoral contact mechanics in an experimental model of osteoarthritis. *J Biomech, 31*(12), 1137-45.

Herzog, W., & Federico, S. (2006). Considerations on joint and articular cartilage mechanics. *Biomechanics and Modeling in Mechanobiology, 5*(2-3), 64-81.

Herzog, W., & Longino, D. (2007). The role of muscles in joint degeneration and osteoarthritis. *J Biomech, 40 Suppl 1*, S54-63.

Hirokawa, S., Solomonow, M., Luo, Z., Lu, Y., & D'Ambrosia, R. (1991). Muscular co-contraction and control of knee stability. *Journal of Electromyography and Kinesiology, 1*(3), 199-208.

Hortobagyi, T., Garry, J., Holbert, D., & Devita, P. (2004). Aberrations in the control of quadriceps muscle force in patients with knee osteoarthritis. *Arthritis Rheum, 51*(4), 562-9.

Hortobagyi, T., Westerkamp, L., Beam, S., Moody, J., Garry, J., Holbert, D., & DeVita, P. (2005). Altered hamstring-quadriceps muscle balance in patients with knee osteoarthritis. *Clin Biomech (Bristol, Avon), 20*(1), 97-104.

Hurley, M. V. (1999). The role of muscle weakness in the pathogenesis of osteoarthritis. *Rheum Dis Clin North Am, 25*(2), 283-98

Hurley, M. V. (2003). Muscle dysfunction and effective rehabilitation of knee osteoarthritis: What we know and what we need to find out. *Arthritis Care and Research, 49*(3), 444-452.

Hurwitz, D. E., Sumner, D. R., Andriacchi, T. P., & Sugar, D. A. (1998). Dynamic knee loads during gait predict proximal tibial bone distribution. *Journal of Biomechanics, 31*(5), 423-430.

Ihn, J. C., Kim, S. J., & Park, I. H. (1993). In vitro study of contact area and pressure distribution in the human knee after partial and total meniscectomy. *International Orthopaedics, 17*(4), 214-218.

Jeffcote, B., Nicholls, R., Schirm, A., & Kuster, M. S. (2007). The variation in medial and lateral collateral ligament strain and tibiofemoral forces following changes in the flexion and extension gaps in total knee replacement: A laboratory experiment using cadaver knees. *Journal of Bone and Joint Surgery - Series B, 89*(11), 1528-1533.

Kainz, H., Reng, W., Augat, P., & Wurm, S. (2011). Influence of total knee arthroplasty on patellar kinematics and contact characteristics. *International Orthopaedics,* , 1-6.

Kamekura, S., Hoshi, K., Shimoaka, T., Chung, U., Chikuda, H., Yamada, T., Kawaguchi, H. (2005). Osteoarthritis development in novel experimental mouse models induced by knee joint instability. *Osteoarthritis and Cartilage, 13*(7), 632-641.

Kessler, M. A., Behrend, H., Henz, S., Stutz, G., Rukavina, A., & Kuster, M. S. (2008). Function, osteoarthritis and activity after ACL-rupture: 11 years follow-up results of conservative versus reconstructive treatment. *Knee Surgery, Sports Traumatology, Arthroscopy, 16*(5), 442-448.

Kettelkamp, D. B., & Jacobs, A. W. (1972). Tibiofemoral contact area--determination and implications. *Journal of Bone and Joint Surgery - Series A, 54*(2), 349-356.

Kostogiannis, I., Ageberg, E., Neuman, P., Dahlberg, L., Fridén, T., & Roos, H. (2007). Activity level and subjective knee function 15 years after anterior cruciate ligament injury: A prospective, longitudinal study of nonreconstructed patients. *American Journal of Sports Medicine, 35*(7), 1135-1143.

Kurosawa, H., Fukubayashi, T., & Nakajima, H. (1980). Load-bearing mode of the knee joint: Physical behavior of the knee joint with or without menisci. *Clinical Orthopaedics and Related Research, NO 149*, 283-290.

Lee, S. J., Aadalen, K. J., Malaviya, P., Lorenz, E. P., Hayden, J. K., Farr, J., . . . Cole, B. J. (2006). Tibiofemoral contact mechanics after serial medial meniscectomies in the human cadaveric knee. *American Journal of Sports Medicine, 34*(8), 1334-1344.

Lequesne, M. G., Dang, N., & Lane, N. E. (1997). Sport practice and osteoarthritis of the limbs. *Osteoarthritis and Cartilage, 5*(2), 75-86.

Lewek, M. D., Ramsey, D. K., Snyder-Mackler, L., & Rudolph, K. S. (2005). Knee stabilization in patients with medial compartment knee osteoarthritis. *Arthritis Rheum, 52*(9), 2845-53.

Lewek, M. D., Rudolph, K. S., & Snyder-Mackler, L. (2004). Quadriceps femoris muscle weakness and activation failure in patients with symptomatic knee osteoarthritis. *Journal of Orthopaedic Research, 22*(1), 110-115.

Lewold, S., Robertsson, O., Knutson, K., & Lidgren, L. (1998). Revision of unicompartmental knee arthroplasty. *Acta Orthopaedica Scandinavica, 69*(5), 469-474.

Li, G., Moses, J. M., Papannagari, R., Pathare, N. P., DeFrate, L. E., & Gill, T. J. (2006a). Anterior cruciate ligament deficiency alters the in vivo motion of the tibiofemoral cartilage contact points in both the anteroposterior and mediolateral directions. *Journal of Bone and Joint Surgery - Series A, 88*(8), 1826-1834.

Li, G., Moses, J. M., Papannagari, R., Pathare, N. P., DeFrate, L. E., & Gill, T. J. (2006b). Anterior cruciate ligament deficiency alters the in vivo motion of the tibiofemoral cartilage contact points in both the anteroposterior and mediolateral directions. *Journal of Bone and Joint Surgery - Series A, 88*(8), 1826-1834.

Li, G., Papannagari, R., DeFrate, L. E., Yoo, J. D., Park, S. E., & Gill, T. J. (2007). The effects of ACL deficiency on mediolateral translation and varus-valgus rotation. *Acta Orthopaedica, 78*(3), 355-360.

Liau, J., Cheng, C., Huang, C., & Lo, W. (2002). The effect of malalignment on stresses in polyethylene component of total knee prostheses - A finite element analysis. *Clinical Biomechanics, 17*(2), 140-146.

Lloyd, D. G., & Buchanan, T. S. (2001). Strategies of muscular support of varus and valgus isometric loads at the human knee. *J Biomech, 34*(10), 1257-67.

Lohmander, L. S., Östenberg, A., Englund, M., & Roos, H. (2004). High prevalence of knee osteoarthritis, pain, and functional limitations in female soccer players twelve years after anterior cruciate ligament injury. *Arthritis and Rheumatism, 50*(10), 3145-3152.

MacWilliams, B. A., Wilson, D. R., Desjardins, J. D., Romero, J., & Chao, E. Y. S. (1999). Hamstrings cocontraction reduces internal rotation, anterior translation, and anterior cruciate ligament load in weight-bearing flexion. *Journal of Orthopaedic Research, 17*(6), 817-822.

Maletsky, L. P., & Hillberry, B. M. (2000). Loading evaluation of knee joint during walking using the next generation knee simulator. *American Society of Mechanical Engineers, Bioengineering Division (Publication) BED, 48*, 91-92.

Maletsky, L. P., & Hillberry, B. M. (2005). Simulating dynamic activities using a five-axis knee simulator. *Journal of Biomechanical Engineering, 127*(1), 123-133.

Manal, K., Gardinier, J., & Chimera, N. (2006). What are we missing when using inverse dynamics? In *Proceedings of the American Society of Biomechanics* (Vol. 30).

Marouane, H.,, Shirazi-Adl, H., Hashemi, J., Quantification of the role of tibial posterior slope in knee joint mechanics and ACL force in simulated gait. Journal of Biomechanics 48 (2015) 1899–1905.

Marzo, J. M., & Gurske-DePerio, J. (2009). Effects of medial meniscus posterior horn avulsion and repair on tibiofemoral contact area and peak contact pressure with clinical implications. *American Journal of Sports Medicine, 37*(1), 124-129.

Matsuda, S., Ishinishi, T., White, S. E., & Whiteside, L. A. (1997). Patellofemoral joint after total knee arthroplasty: Effect on contact area and contact stress. *Journal of Arthroplasty, 12*(7), 790-797.

Morimoto, Y., Ferretti, M., Ekdahl, M., Smolinski, P., & Fu, F. H. (2009). Tibiofemoral joint contact area and pressure after single- and double-bundle anterior cruciate ligament reconstruction. *Arthroscopy - Journal of Arthroscopic and Related Surgery, 25*(1), 62-69.

Müller, O., Lo, J., Wünschel, M., Obloh, C., & Wülker, N. (2009). Simulation of force loaded knee movement in a newly developed in vitro knee simulator. [Simulation von belastungsabhängigen Kniebewegungen in einem neuartigen Knie-Simulator für In-vitro-Studien] *Biomedizinische Technik, 54*(3), 142-149.

Mündermann, A., Dyrby, C. O., D'Lima, D. D., Colwell Jr., C. W., & Andriacchi, T. P. (2008). In vivo knee loading characteristics during activities of daily living as measured by an instrumented total knee replacement. *Journal of Orthopaedic Research, 26*(9), 1167-1172.

Paci, J. M., Scuderi, M. G., Werner, F. W., Sutton, L. G., Rosenbaum, P. F., & Cannizzaro, J. P. (2009). Knee medial compartment contact pressure increases with release of the type i anterior intermeniscal ligament. *American Journal of Sports Medicine, 37*(7), 1412-1416.

Perillo-Marcone, A., & Taylor, M. (2007). Effect of varus/valgus malalignment on bone strains in the proximal tibia after TKR: An explicit finite element study. *Journal of Biomechanical Engineering, 129*(1), 1-11.

Peters, A., Galna, B., Sangeux, M., Morris, M., & Baker, R. (2010). Quantification of soft tissue artifact in lower limb human motion analysis: A systematic review. *Gait and Posture, 31*(1), 1-8.

Poh, S., Yew, K., A., Wong, P., K., Koh, S., J., Chia, S., Fook-Chong, S., & Howe, T. (2012). Role of the anterior intermeniscal ligament in tibiofemoral contact mechanics during axial joint loading. *Knee,* 19, (2), p 135-139

L. G. Portney and M. P. Watkins, *Foundations of Clinical Research: Applications to Practice*. Prentice Hall, 2000Radin, E. L., Swann, D. A., Paul, I. L., & McGrath, P. J. (1982). Factors influencing articular cartilage wear in vitro. *Arthritis and Rheumatism, 25*(8), 974-980.

Radin, E. L., Yang, K. H., Riegger, C., Kish, V. L., & O'Connor, J. J. (1991). Relationship between lower limb dynamics and knee joint pain. *Journal of Orthopaedic Research, 9*(3), 398-405.

Rajendran, K. (1985). Mechanism of locking at the knee joint. *J. Anat.* 143, 189–194.

Ramsey, D. K., Snyder-Mackler, L., Lewek, M., Newcomb, W., & Rudolph, K. S. (2007). Effect of anatomic realignment on muscle function during gait in patients with medial compartment knee osteoarthritis. *Arthritis Care and Research, 57*(3), 389-397.

Youssef, A R., Longino, D., Seerattan, R., Leonard, T., & Herzog, W. (2009). Muscle weakness causes joint degeneration in rabbits. *Osteoarthritis Cartilage, 17*(9), 1228-35.

Riegger-Krugh, C., Gerhart, T. N., Powers, W. R., & Hayes, W. C. (1998). Tibiofemoral contact pressures in degenerative joint disease. *Clinical Orthopaedics and Related Research,* (348), 233-245.

Ryan, J., Magnussen, RA., Cox, CL (2014). ACL Reconstruction: Do Outcomes Differ by Sex? A Systematic Review. JBJS, 96 (6), 507 -512

Schipplein, O. D., & Andriacchi, T. P. (1991). Interaction between active and passive knee stabilizers during level walking. *Journal of Orthopaedic Research, 9*(1), 113-119.

Seo, J., Li, G., Shetty, G., M., Kim, J., Bae, J., Jo, M., Nha, K. (2009). Effect of repair of radial tears at the root of the posterior horn of the medial meniscus with the pullout suture technique: A biomechanical study using porcine knees. *Arthroscopy - Journal of Arthroscopic and Related Surgery, 25*(11), 1281-1287.

Shaw, J. A., & Murray, D. G. (1973). Knee joint simulator. Clin. Orthop. *no.94*, 15-23.

Shelburne, K. B., Torry, M. R., & Pandy, M. G. (2006). Contributions of muscles, ligaments, and the ground-reaction force to tibiofemoral joint loading during normal gait. *J Orthop Res, 24*(10), 1983-90.

Sokoloff L, (1963). The biology of degenerative disease. *Perspectives in Biology and Medicine, 42*, 94-106.

Solomonow, M., Baratta, R., Shoji, H., & D'Ambrosia, R. D. (1986). The myoelectric signal of electrically stimulated muscle during recruitment: An inherent feedback parameter for a closed-loop control scheme. *IEEE Trans Biomed Eng, 33*(8), 735-45.

Stewart, T., Jin, Z. M., Shaw, D., Auger, D. D., Stone, M., & Fisher, J. (1995). Experimental and theoretical study of the contact mechanics of five total knee joint replacements. *Proceedings of the Institution of Mechanical Engineers, Part H: Journal of Engineering in Medicine, 209*(4), 225-231.

Szklar, O., & Ahmed, A. M. (1987). Simple unconstrained dynamic knee simulator. *Journal of Biomechanical Engineering, 109*(3), 247-251.

Tashman, S., Collon, D., Anderson, K., Kolowich, P., & Anderst, W. (2004). Abnormal rotational knee motion during running after anterior cruciate ligament reconstruction. *American Journal of Sports Medicine, 32*(4), 975-983.

Taylor, S. J. G., & Walker, P. S. (2001). Forces and moments telemetered from two distal femoral replacements during various activities. *Journal of Biomechanics, 34*(7), 839-848.

Van De Velde, S. K., Bingham, J. T., Hosseini, A., Kozanek, M., DeFrate, L. E., Gill, T. J., & Li, G. (2009). Increased tibiofemoral cartilage contact deformation in patients with anterior cruciate ligament deficiency. *Arthritis and Rheumatism, 60*(12), 3693-3702.

Varadarajan, K. M., Moynihan, A. L., D'Lima, D., Colwell, C. W., & Li, G. (2008). In vivo contact kinematics and contact forces of the knee after total knee arthroplasty during dynamic weight-bearing activities. *Journal of Biomechanics, 41*(10), 2159-2168.

Wallace, A. L., Harris, M. L., Walsh, W. R., & Bruce, W. J. M. (1998). Intraoperative assessment of tibiofemoral contact stresses in total knee arthroplasty. *Journal of Arthroplasty, 13*(8), 923-927.

Werner, F. W., Ayers, D. C., Maletsky, L. P., & Rullkoetter, P. J. (2005). The effect of valgus/varus malalignment on load distribution in total knee replacements. *Journal of Biomechanics, 38*(2), 349-355.

Whiteside, L. A., Kasselt, M. R., & Haynes, D. W. (1987). Varus-valgus and rotational stability in rotationally unconstrained total knee arthroplasty. *Clinical Orthopaedics and Related Research, No. 219*, 147-157.

Williams, G. N., Chmielewski, T., Rudolph, K., Buchanan, T. S., & Snyder-Mackler, L. (2001). Dynamic knee stability: Current theory and implications for clinicians and scientists. *The Journal of Orthopaedic and Sports Physical Therapy, 31*(10), 546-566.

Wilson, D. R., Apreleva, M. V., Eichler, M. J., & Harrold, F. R. (2003). Accuracy and repeatability of a pressure measurement system in the patellofemoral joint. *Journal of Biomechanics, 36*(12), 1909-1915.

Woo, S. L., Abramowitch, S. D., Kilger, R., & Liang, R. (2006). Biomechanics of knee ligaments: Injury, healing, and repair. *Journal of Biomechanics, 39*(1), 1-20.

Wu, J. Z., Herzog, W., & Epstein, M. (2000). Joint contact mechanics in the early stages of osteoarthritis. *Med Eng Phys, 22*(1), 1-12.

Wünschel, M., Leichtle, U., Obloh, C., Wülker, N., & Müller, O. (2011). The effect of different quadriceps loading patterns on tibiofemoral joint kinematics and patellofemoral contact pressure during simulated partial weight-bearing knee flexion. *Knee Surgery, Sports Traumatology, Arthroscopy, 19*(7), 1099-1106.

Yao, J. Q., & Seedhom, B. B. (1991). New technique for measuring contact areas in human joints. the '3S technique'. *Proceedings of the Institution of Mechanical Engineers, Part H: Journal of Engineering in Medicine, 205*(2), 69-72.

Yoo, J. D., Papannagari, R., Park, S. E., DeFrate, L. E., Gill, T. J., & Li, G. (2005). The effect of anterior cruciate ligament reconstruction on knee joint kinematics under simulated muscle loads. *American Journal of Sports Medicine, 33*(2), 240-246.

Zatsiorsky and Prilutsky. (2012). Biomechanics of skeletal muscles. Human Kinetics, USA, p 255-256.